

2015

## Characterization of STARD4 and STARD6 Proteins in Human Ovarian Tissue and Human Granulosa Cells and Cloning of Human STARD4 Transcripts

Aisha Shaaban  
*University of South Carolina*

Follow this and additional works at: <https://scholarcommons.sc.edu/etd>



Part of the [Biomedical and Dental Materials Commons](#), and the [Other Medical Sciences Commons](#)

---

### Recommended Citation

Shaaban, A.(2015). *Characterization of STARD4 and STARD6 Proteins in Human Ovarian Tissue and Human Granulosa Cells and Cloning of Human STARD4 Transcripts*. (Master's thesis). Retrieved from <https://scholarcommons.sc.edu/etd/3723>

This Open Access Thesis is brought to you by Scholar Commons. It has been accepted for inclusion in Theses and Dissertations by an authorized administrator of Scholar Commons. For more information, please contact [digres@mailbox.sc.edu](mailto:digres@mailbox.sc.edu).

**Characterization of STARD4 and STARD6 Proteins in Human Ovarian Tissue and  
Human Granulosa Cells and Cloning of Human STARD4 Transcripts**

By

Aisha Shaaban

Bachelor of Medicine and General Surgery  
Tripoli University, 2008

---

Submitted in Partial Fulfillment of the Requirements

For the Degree of Master of Science in

Biomedical Science

School of Medicine

University of South Carolina

2015

Accepted by:

Holly LaVoie, Director of Thesis

Edie Goldsmith, Reader

Kenneth Walsh, Reader

Lacy Ford, Senior Vice Provost and Dean of Graduate Studies

© Copyright by Aisha Shaaban, 2015

All Rights Reserve

## **Dedication**

To my lovely husband Najmeddin Rughaei. For your encouragement, support, love, and patience. For taking good care of me and our little daughter Jana.

To my parents, I am who I am today because of your encouragement and continuous support in every way.

## **Acknowledgments**

First of all, I would like to thank my mentor Dr. Holly A. LaVoie for your education and direction in every step during my training in your lab. Also I would like to thank you for your patience and understanding when I was suffering from health problems and for that I will be grateful forever. I would like also to thank each of my committee members for your time, advice, and expertise: Dr. Edie Goldsmith, and Dr. Ken Walsh. I would like to thank individually Nawal Yahya for assisting with the RNA isolation and Real-time PCR for human tissue samples, and for teaching me and helping me to perform Western blots for the human tissues. I would like to thank Dr. Robert L. Price and Anna McNeal of the Instrumentation Resource Facility (IRF) for teaching me fluorescent staining and confocal imaging. I would like to thank Richard Kordus from and Dr. Gail Whitman-Elisa from Advanced Fertility and Reproductive Endocrinology Institute, LLC in West Columbia, SC, for providing human luteinized granulosa cells from patients to our laboratory.

## Abstract

Progesterone is essential hormone for pregnancy, which is produced by the human corpus luteum in early pregnancy until the placenta assumes this function. Transport of the cholesterol from the outer to the inner mitochondrial membrane is the rate limiting step for the *de novo* synthesis of pregnenolone (the precursor to progesterone), a process mediated by STARD1. STARD1 contains a C-terminal lipid binding domain which binds cholesterol and an N-terminal domain targeting STARD1 to the mitochondrial membrane. Unlike STARD1, STARD4 and STARD6 proteins lack a mitochondrial targeting sequence; however, they can bind cholesterol and increase steroidogenesis in model systems. In this study, we found both STARD4 and STARD6 mRNA expression in all steroidogenic compartments of human ovarian tissue. Western blots of human ovarian tissue demonstrated STARD4 and STARD6 immunoreactive protein at approximate molecular mass of 30 kDa and 43 kDa, respectively. Microscopically, STARD4 and STARD6 proteins are localized to steroidogenic cells of ovarian follicles (in granulosa and theca cells) and luteal cells. In order to determine the actual protein mass for ovarian STARD4, mRNA from human luteinized granulosa cells (hLGC), we aimed to clone all major transcripts of STARD4 from a cDNA library we generated from granulosa cell poly (A) RNA. Two major transcripts were isolated for STARD4. First one possessing all six exons with a small variation of 6 nucleotides in the untranslated exon 1 was predicted to yield a full-length protein of 205 aa.

The second transcript possessed an exon 4 deletion, which introduced a premature stop codon and is predicted to yield a truncated protein with sizes of either 55 amino acids or 107 amino acids. Both cDNAs were placed in expression vectors. The full-length recombinant STARD4 protein appeared on Western blot at an approximate size of 24 kDa. Using the COS cell F2-steroidogenic assay, transfected full-length and exon 4-deleted transcript protein functions were compared. Full-length STARD4 protein was able to increase the pregnenolone production significantly compared to empty vector, whereas truncated (exon 4 deleted) STARD4 was not. Although full-length STARD4 has the potential to increase steroidogenesis, it is unlikely that the truncated protein has similar ability.

## Table of Contents

Dedication.....	iii
Acknowledgments.....	iv
Abstract.....	v
List of Figures.....	x
List of Abbreviations.....	xi
Chapter I: Introduction.....	1
1.1 Introduction overview.....	1
1.2 Anatomy of female reproductive system.....	1
1.3 Physiology of ovulation and menstrual cycle.....	4
1.4 Cholesterol homeostasis.....	6
1.5 Steroidogenesis and regulation.....	8
1.6 START domain protein family.....	11
1.7 STARD4 regulation.....	15
1.8 STARD4 gene.....	17

1.9 STARD6 protein .....	18
1.10 Diseases related to START proteins and steroid production.....	18
1.11 Aims of this study .....	20
Chapter II: Materials and Methods .....	22
2.1 Human granulosa cell isolation .....	22
2.2 Protein isolation .....	23
2.3 Protein quantification.....	24
2.4 SDS-polyacrylamide gel electrophoresis and immunoblotting.....	24
2.5 Western blot.....	25
2.6 Stripping immunoblots .....	26
2.7 RNA isolation and cDNA synthesis .....	27
2.8 Real-time PCR.....	28
2.9 Immunofluorescent labeling of STARD4 for confocal imaging.....	30
2.10 Confocal imaging.....	31
2.11 Immunohistochemistry .....	31
2.12 Cloning of human STARD4 transcripts .....	33
2.13 COS-1 cells culture.....	36

2.14 COS-F2 steroidogenic assay .....	36
2.15 Luciferase assay.....	37
2.16 Pregnenolone ELISA assay .....	38
2.17 Data analysis .....	39
Chapter III: Results .....	40
3.1 Detection of STARD4 and STARD6 mRNAs and proteins in human ovarian tissues.....	40
3.2 Subcellular localization of STARD4 in transfected COS-1 cells by immunofluorescence microscopy .....	43
3.3 Human luteinized granulosa cells express multiple STARD4 mRNA transcripts.....	43
3.4 Determining the size of recombinant proteins produced from human full-length STARD4 and exon four-deleted STARD4 mRNA isolated from hGC .....	44
3.5 Human full-length STARD4 recombinant protein is able to facilitate de novo steroidogenesis in the COS-1 F2 assay .....	46
Chapter IV: Discussion .....	62
References.....	69
Appendix.....	76
Appendix A: Permission to reuse figure 1.2 .....	76

## List of Figures

Figure 1.1. The ovary demonstrating different stages of follicular development.....	3
Figure 1.2. Steroidogenic pathway .....	12
Figure 3.1. STARD4 and STARD6 mRNA expression in human ovarian tissues.....	47
Figure 3.2. Western blot analysis of STARD4 and STARD6 proteins in human ovarian tissue samples .....	48
Figure 3.3. Immunolocalization of STARD4 and STARD6 in human ovarian tissue section .....	49
Figure 3.4. Immunolocalization of STARD4 and STARD6 proteins in human antral follicles .....	50
Figure 3.5. Immunolocalization of STARD4 and STARD6 in the corpus luteum of human ovarian tissues.....	51
Figure 3.6 Immunolocalization of STARD4 and STARD6 in corpus luteum of human ovarian tissues.....	52
Figure 3.7. Immunolocalization of STARD4 and STARD6 in human ovarian tissue sections.....	53
Figure 3.8. Immunofluorescence confocal microscopy assessment of recombinant STARD4 and endogenous GRP78 proteins in transfected COS-1 cells.....	54
Figure 3.9. Schematic view of the major mRNA transcripts of human STARD4 which were isolated from human granulosa cells with their sizes on agarose gel ....	55
Figure 3.10. The homology and the alignment of STARD4-WT and STARD4 cDNA.....	56
Figure 3.11. Diagram illustrating the predicted sizes of STARD4 wild-type and truncated proteins and their alignment with Homo sapiens STARD4 protein.....	58
Figure 3.12. Western blot for comparing human recombinant STARD4 and endogenous STARD4 proteins .....	60
Figure 3.13. COS-F2 steroidogenic assay to assess the pregnenolone production by recombinant STARD4 derived from human granulosa cells transcripts.....	61

## List of Abbreviations

3 $\beta$ -HSD .....	3beta-hydroxysteroid dehydrogenase
ACAT .....	acyl-coenzyme A: cholesterol acyl transferase
ACTH .....	adrenocorticotropin hormone
BSA .....	serum albumin protein
C/EBP .....	CCAAT/enhancer-binding protein
CAH .....	Lipoid Congenital Adrenal Hyperplasia
cAMP .....	cyclic adenosine mono-phosphate
CH .....	corpus hemorrhagicum
CL .....	corpus luteum
CRE .....	cAMP response element
CRH .....	corticotropin releasing hormone
DAB .....	3,3-diaminobenzidine
DAPI .....	4',6-diamidine-2-phynylindole dihydrochloride
DHEA .....	dehydroepiandrosterone

DOR ..... Diminished Ovarian Reserve

D-PBS ..... Dulbecco's phosphate buffer saline

ER ..... endoplasmic reticulum

FBS ..... fetal bovine serum

FSH ..... follicle stimulating hormone

GAR ..... goat anti-rabbit

GF-I ..... insulin-like growth factors I

GRP78 ..... Glucose-regulated protein 78

HDL ..... high density lipoprotein

HMGC<sub>o</sub>A ..... 3-hydroxy-3-methylglutaryl co-enzyme A

HMGR ..... hydroxyl methyl glutaryl-CoA reductase

HRP ..... Horseradish Peroxidase conjugate solutions

HSL ..... hormone sensitive lipase

IGF- II ..... insulin-like growth factors II

IMM ..... inner mitochondria membrane

LB Broth ..... Lennox Broth base media

LDH ..... low density lipoprotein

LH ..... Luteinizing hormone

LTPs ..... lipid-transfer proteins

LXR ..... liver X receptor

MAM ..... mitochondrial-associated ER membrane

MCSs ..... membrane contact sites

NAFLD ..... non-alcoholic fatty liver diseases

OSBP ..... oxysterol-binding protein

P450<sub>scc</sub> ..... cytochrome P450 side chain cleavage enzyme

PCOS ..... polycystic ovarian syndrome

PKA ..... protein kinase A

PKC ..... protein kinase C

POI ..... primary ovarian insufficiency

PTMs ..... posttranslational modifications

SDS ..... sodium dodecyl sulfate

SF-1 ..... steroidogenic factor 1

SR-B1 ..... scavenger receptor B1

SREBP ..... sterol regulatory element-binding protein

SREs..... sterol regulatory elements

StAR..... steroidogenic acute regulatory protein

STARD1 .....START domain protein 1

STARD4 .....START domain protein 4

STARD6 .....START domain protein 6

START..... The steroidogenic acute regulatory protein-related lipid transfer proteins

TBS ..... Tris buffered saline

TTBS..... TBS-Tween

VDAC2 .....voltage-dependent anion channel 2

WCE..... Whole cell extract

# **Chapter I**

## **Introduction**

### **1.1 Introduction overview**

Infertility is a critical problem all over the world among couples. According to the American Society for Reproductive Medicine, infertility is defined by the failure to achieve a successful pregnancy after twelve months or more of appropriate, timed unprotected intercourse or therapeutic donor insemination (Definitions of Infertility and Recurrent Pregnancy Loss: A Committee Opinion. 2013). Around 42 million couples of reproductive age worldwide were affected by infertility in 1990, with the prevalence of infertility in 2010 being increased to 48.5 million (Mascarenhas et al. 2012). In the United States around 15% of couples of reproductive age suffer from infertility (DeAngelis et al. 2014). Infertility has different etiologies including male factors and female factors. The causes of infertility in females are varied and can be either structural (fallopian tubes, uterus) or functional (ovary, hypothalamic-pituitary origin). Ovulation disorders are the most common of female infertility disorders and include polycystic ovarian syndrome (PCOS), primary ovarian insufficiency (POI), and premature ovarian failure (Infertility Reproductive Health CDC 2015).

### **1.2 Anatomy of the female reproductive system**

The female reproductive system anatomically consists of internal reproductive organs and external genitalia. The internal reproductive organs include two ovaries, one uterus with two extended tubes, which are known as Fallopian tubes, and the vagina.

Each ovary is located in the ovarian fossa relative to the lateral side of the pelvic wall and connected to the uterus by its broad ligament on both sides and the ovarian ligament. The ovaries are grayish-pink in color with length of 4 cm, width of 2 cm, and thickness of 8 mm. The uterine tubes are curved on the upper border of broad ligament above the ovaries, then arched downward with finger-like extensions called fimbria toward the ovary. Histologically, the surface of the ovary is covered by squamous to columnar epithelial cells, and this layer of cells is called the germinal epithelium. The internal portion of the ovary is composed of ovarian follicles embedded into a stromal network; where the stroma consists of connective tissue fibers and cells. Near the ovarian surface, there is a thick white layer of stroma called the tunica albuginea (Henry 2000).

Internally, the ovarian follicles, with variant size, are arranged in between outer cortical and inner medullary regions. Post-pubertally almost each follicle goes through the same developmental stages starting from primordial follicles and enlarging to form antral follicles (Figure 1.1). Only few follicles fully mature to the Graafian follicle stage. The primordial follicle is composed of one oocyte encircled by one or more layers of epithelial cells (follicular cells). During fetal life, primordial follicles are formed from a primary oocyte surrounded by a single layer of flat follicular cells. By puberty, most of primary follicles have undergone a degenerative process called atresia, and about only 300,000 oocytes remain. At various times a group of follicles start to develop and produce a mature follicle. By mechanisms not fully understood, periodically primordial follicles are activated and the oocyte grows and the flat epithelium cells morphologically change into simple cuboidal epithelium to form a unilaminar primary follicle. The next stage is the multilaminar primary follicle, where the follicular cells continue to divide and

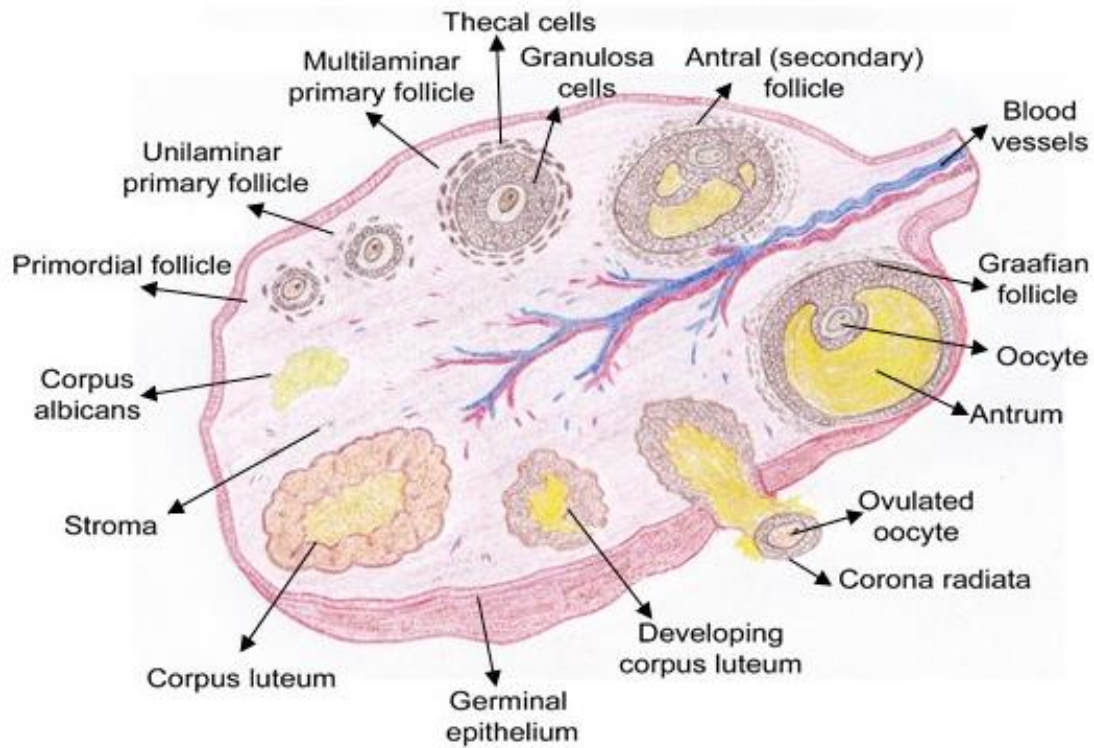


**Figure 1.1. The ovary demonstrating different stages of follicular development.** Schematic drawing of the developmental stages of ovarian follicles, beginning with the primordial follicle and ending with the pre-ovulatory or Graafian follicle. After the oocyte is ovulated, the residual cells of the follicle become luteal cells and will transform into the corpus luteum. If pregnancy is not established the corpus luteum will regress forming the corpus albicans. (Based on information from Junqueira's Basic Histology, Mescher, 2013).

form multiple layers of granulosa cells around the growing oocyte. The zona pellucida develops between the oocyte and granulosa cell layers, which is an extracellular material consisting mainly of glycoproteins secreted by the oocyte (Mescher 2013).

The antral or secondary follicle is the third stage of follicular development, where the follicle increases in size and creates small cavities between the granulosa cells layer by their follicular fluid secretions. The granulosa cells rearrange to produce one larger cavity called an antrum filled with follicular fluid. The follicular fluid contains estrogens, progesterone, and androstenedione. The follicular fluid also contains plasminogen, fibrinogen, heparin sulfate proteoglycan, hyaluronate, and growth factors such as insulin-like growth factors. The stromal cells that surround the follicle proliferate and differentiate into two distinct layers, the theca externa and the theca interna. Thecal cells produce the androgen hormone androstenedione, which is transported into granulosa cells and converted into estrogen hormone. In humans one antral follicle is selected to be dominant and grows to form a mature follicle called a Graafian follicle (Mescher 2013).

### **1.3 Physiology of ovulation and menstrual cycle**

In order to understand reproductive diseases, we need to understand physiology of female reproductive system, the ovulation process, and the cyclical changes that occur in the ovary. Ovulation is a physiological cyclic event which occurs in most reproductive age women on a monthly basis. Ovulation occurs under the influence of both follicle stimulating hormone (FSH) and luteinizing hormone (LH) from the anterior pituitary gland. Beginning at puberty and at regular intervals, there is activation of some of the resting follicle pool, over 2-3 months these follicles grow to reach the final maturation stage. During each menstrual cycle, only one follicle is chosen to continue to grow into a

large dominant Graafian follicle. The preovulatory (Graafian) follicle ovulates at the middle of each menstrual cycle, and the remnants of ovulated follicle undergoes luteinization to form a corpus luteum, which produces a large amount of progesterone within few days after ovulation.

The maturing ovarian follicle is composed of an oocyte surrounded by granulosa cells and theca cells with a fluid filled antrum in the granulosa cell layers. During the antral follicle stage, the thecal cells have steroidogenic activity under the influence of LH, where they synthesize androgens, androstenedione and testosterone. On the other hand, the granulosa cells of more advanced follicles have abundant of FSH receptors and high sensitivity to FSH which in turn upregulates the gene expression of CYP19 (aromatase) and LH receptors; eventually, the granulosa cells of selected follicles utilize aromatase to convert the diffused androstenedione into estrone and testosterone into estradiol. The large Graafian follicle produces abundant estrogen that subsequently leads to the LH surge and ovulation of the oocyte, leaving the granulosa and theca cells within the ovary to luteinize enabling them to dramatically increase the *de novo* steroidogenesis during the luteal phase (White 2013).

After ovulation, the luteinized granulosa and theca, or luteal cells now have dramatically increased capacity to make the first steroid hormone pregnenolone from its primary precursor, cholesterol. Enzymes of luteal cells convert pregnenolone to progesterone and estrogens, however, progesterone is the main steroid hormone produced by luteal cells.

#### **1.4 Cholesterol homeostasis**

Lipids have various forms with different functions; however, they share the same feature of lacking water solubility. At the level of the organism, lipids serve as energy storage or hormones mediators. While at the cellular level, lipids provide structural components of cell membranes and the membranes of cellular organelles. The major type of lipids are glycerolipids (glycerol and three fatty acids), sphingolipids (sphingosine, fatty acid and choline or mono- or oligo- saccharide), and sterols such as cholesterol (Alpy and Tomasetto 2014). Cholesterol is an essential structural molecule in cell membranes of eukaryotic cells, where it comprises around 30% of the plasma membrane total lipid molecules (Ikonen 2008). In addition, cholesterol is the precursor substrate for steroid hormones biosynthesis in the gonads (ovaries and testis), adrenal gland, and placenta. In addition, some central nervous system cells can make steroids (Furukawa et al. 1998). Cholesterol serves also as a precursor molecule for bile acid formation in the liver and vitamin D biosynthesis in the kidneys. The human body derives cholesterol either from diet or/and by *de novo* synthesis (Ikonen 2008); in addition, cholesterol homeostasis is maintained through its cellular uptake, transport/trafficking, sorting, biosynthesis, storage, secretion, and catabolism into bile acids (Pandak et al. 2001). Different lipid types, including cholesterol, are distributed variously between cell membrane and other compartments (Du et al. 2015); where the endoplasmic reticulum (ER), a major site of cholesterol synthesis and regulation, has the lowest cholesterol content, around 5% of lipid molecule; while, the cell membrane has the highest cholesterol contents (Ikonen 2008; Radhakrishnan et al. 2008).

Cholesterol level is tightly controlled via the feedback pathway of sterol regulatory element-binding protein transcription factors (SREBP). SREBP is membrane-bound transcription factors on the endoplasmic reticulum. When the ER level of sterol is low, the SREBP precursor is cleaved and transferred to the Golgi complex, where it is transformed into its active soluble form, which migrates into the nucleus. In the nucleus, SREBP increases the gene expression for proteins responsible for cholesterol synthesis and uptake (Reinhart et al. 1987; Goldstein et al. 2006).

Intracellular cholesterol trafficking occurs by different mechanisms including vesicular transport or/and non-vesicular transport; both transport types maintain the heterogeneous distribution of cholesterol between the membranes of cellular organelles (Prinz 2002). In the non-vesicular transport, the lipid transport between adjacent membranes occurs via specific domains of a variety of lipid-transfer proteins (LTPs). This process has a huge impact on intracellular lipid trafficking and distribution; however, the underlying mechanism is still an area of active research (Lev 2010). Lipid-transfer proteins move the lipid between two organelles at membrane contact sites (MCSs), where the distance between the two apposed membranes is less than 30 nm. The MCS has specific domains of lipid-transfer proteins to exchange and shuttle lipids such as cholesterol and signals such as calcium between intracellular organelles back and forth through the cytoplasm (Levine 2004; Helle et al. 2013).

Since the endoplasmic reticulum is the main site of lipid synthesis, it forms MCSs thereby networking with associated membranes such as the plasma membrane, and membranes of the mitochondria, Golgi, and lysosomes. This MCS network is involved in lipid transfer and signaling (Levine 2004; Toulmay and Prinz 2011). Mitochondrial-

associated ER membrane (MAM) is a MCS between the endoplasmic reticulum and mitochondrial membranes, where the distance is vary from 10 nm to 60 nm. Vance's group was the first group to characterize the mitochondria-associated membrane fraction or 'ER sub-fraction associated with mitochondria' in rat liver (Vance 1990; Achleitner et al. 1999; Lebiedzinska et al. 2009). This mitochondrial fraction has a high similarity to rough and smooth endoplasmic reticulum and possesses typical ER housekeeping proteins. Indeed, the MAM fraction has several lipid-synthesizing enzymes observed in the ER, including diacylglycerol acyltransferase and acyl-Coenzyme A: cholesterol acyl transferase (ACAT), which indicate that the MAM has a role in lipid synthesis and metabolism (Rusiñol et al. 1994; Vance 2003; Levine 2004).

Oxysterol-binding protein (OSBP) is a novel example of lipid-binding protein at MCSs, which facilitates cholesterol movement between organelle membranes coupled with phosphatidylinositol 4-phosphate (Du et al. 2015). In steroidogenic cells, steroidogenic acute regulatory protein (StAR or STARD1) is the lipid-transfer protein that facilitates cholesterol transfer from the outer-mitochondrial membrane to the inner-mitochondrial membrane (Stocco 2000). A recent study has found that StAR interacts via its C-terminus with a voltage-dependent anion channel 2 (VDAC2) at MAM fraction. They have found the absence of VDAC2 will inhibit steroidogenesis by reducing StAR maturation and processing into the mitochondria. The MAM fraction plays a central role in transferring StAR into the mitochondria (Prasad et al. 2014).

### **1.5 Steroidogenesis and regulation**

Steroidogenesis is the process of synthesizing steroid hormones in a specific cell type, called steroidogenic cells, which is reside in specialized organs (Miller and Auchus

2011). Some examples of steroidogenic cells are: ovarian theca cells which produce androgen, ovarian granulosa cells which convert androgens to estradiol, luteal cells of ovarian corpus luteum and placental syncytiotrophoblasts which synthesize and secrete progesterone, and testicular Leydig cells which make testosterone. Further examples of steroid hormones are glucocorticoids, which are secreted from adrenal fasciculata cells, and mineralocorticoids secreted from adrenal glomerulosa cells (Stocco 2001). In addition, there are neurosteroids produced in the brain, which stimulate or inhibit GABAergic neurons (Majewska et al. 1986). All steroid hormones are important for homeostasis, to manage stressful situations, regulate blood pressure, and the reproduction in all vertebrates including spermatogenesis in males, ovulation and the maintenance of the pregnancy in females.

Steroidogenesis is regulated by anterior-pituitary hormones, ACTH (adrenocorticotropin hormone) stimulates the synthesis of steroid hormones from the adrenal gland. FSH and LH stimulate the synthesis of reproductive hormones, such as estrogen and progesterone from the ovary, and testosterone from testes. The regulation of steroidogenesis has two phases, acute and chronic regulation. The acute phase occurs in response to stimuli with the rapid production of steroid hormones within minutes. While the chronic of steroidogenesis results from the increased synthesis of new steroidogenic pathway enzymes (Miller 1988; Simpson et al. 1992; Stocco and Clark 1996; Stocco 2001).

ACTH, FSH and LH increase the level of cyclic adenosine mono-phosphate (cAMP) in steroidogenic cells of adrenal glands and gonads. Subsequently, cAMP stimulates hormone sensitive lipase (HSL), which hydrolyzes esterified cholesterol, and

inhibits ACAT, which is responsible for esterification of free cholesterol. By stimulating HSL and inhibiting of ACAT, increased intracellular free cholesterol level will be available for steroid hormones synthesis (Papadopoulos and Miller 2012). The steroidogenic cells maintain intracellular cholesterol levels either by uptake of lipoprotein derived cholesterol from high density lipoproteins (HDL) via scavenger receptor B1 (SR-B1), or low density lipoprotein (LDL) via receptor-mediated endocytosis, where LDL attaches to LDL receptors on the cell surface and is internalized. ACTH and LH upregulate LDL receptors and stimulate *de novo* synthesis of cholesterol from acetyl Co A in the endoplasmic reticulum by stimulating 3-hydroxy-3-methylglutaryl co-enzyme A (HMGCoA) reductase, which is the rate-limiting enzyme in cholesterol synthesis ( Miller and Bose 2011; Papadopoulos and Miller 2012; DeAngelis et al. 2014). All these process, in addition to hydrolysis of stored cholesterol esters by hormone sensitive lipase enzyme, provide the cholesterol substrate for initial steroid hormones synthesis (Kraemer et al. 1991).

When the cholesterol is available for steroid synthesis, cholesterol is somehow transferred to StAR on the outer mitochondrial membrane. Cholesterol binds to the carboxyl terminus of StAR protein and is transferred to the inner mitochondrial membrane (IMM). Cholesterol is then cleaved by cytochrome P450 side chain cleavage enzyme (P450<sub>scc</sub>) complex at the IMM to form the first steroid hormone pregnenolone. The complex is made of P450<sub>scc</sub>, adrenodoxin, and adrenodoxin reductase. Cytochrome P450<sub>scc</sub> enzyme is encoded by the CYP11A1 gene and it is officially named CYP11A1 protein. Cyclic AMP is induces P450<sub>scc</sub> expression in the cortex of the adrenal gland (John et al. 1986), and in the ovary and testis (Mellon and Vaisse 1989), leading to

upregulation of steroidogenesis. Regardless of steroidogenic tissue type, transferring and cleaving the cholesterol are the rate-limiting steps in *de novo* steroidogenesis (Papadopoulos and Miller 2012; Stocco 2000). Understanding the trafficking of cholesterol to the outer mitochondrial membrane is an area of active research by many laboratories because it is poorly understood and may involve other proteins related to StAR.

After the first steroid hormone (pregnenolone) is made, it is converted to progesterone either inside the mitochondria by 3beta-hydroxysteroid dehydrogenase (3 $\beta$ -HSD, mitochondrial form), or outside the mitochondria in the microsomal compartment-ER (Figure 1.2) (Cherradi et al. 1994; Cherradi et al. 1995). The following steps in the steroidogenesis are regulated by several P450 enzymes such as, 17 $\alpha$ -hydroxylase (P450c17/CYP17A1), which converts pregnenolone sequentially to dehydroepiandrosterone (DHEA) in combination with its 17,20-lyase activity. Also, it converts progesterone sequentially into androstenedione in androgenic tissue. CYP19A1 (aromatase) in granulosa cells, which converts androstenedione to estradiol (White 2013).

### **1.6 START domain protein family**

The steroidogenic acute regulatory protein-related lipid transfer proteins (START) have domains that bind and facilitate lipids transport intracellularly. The START domain modeled after the prototype StAR has approximately 210 amino acids in a globular structure of a beta sheet core and an outer surface of alpha helices. This organization of beta sheet and alpha helices results in a hydrophobic cavity on the internal surface for lipid binding, where the lipid binds to the carboxy-terminal of the alpha helix. A subset of

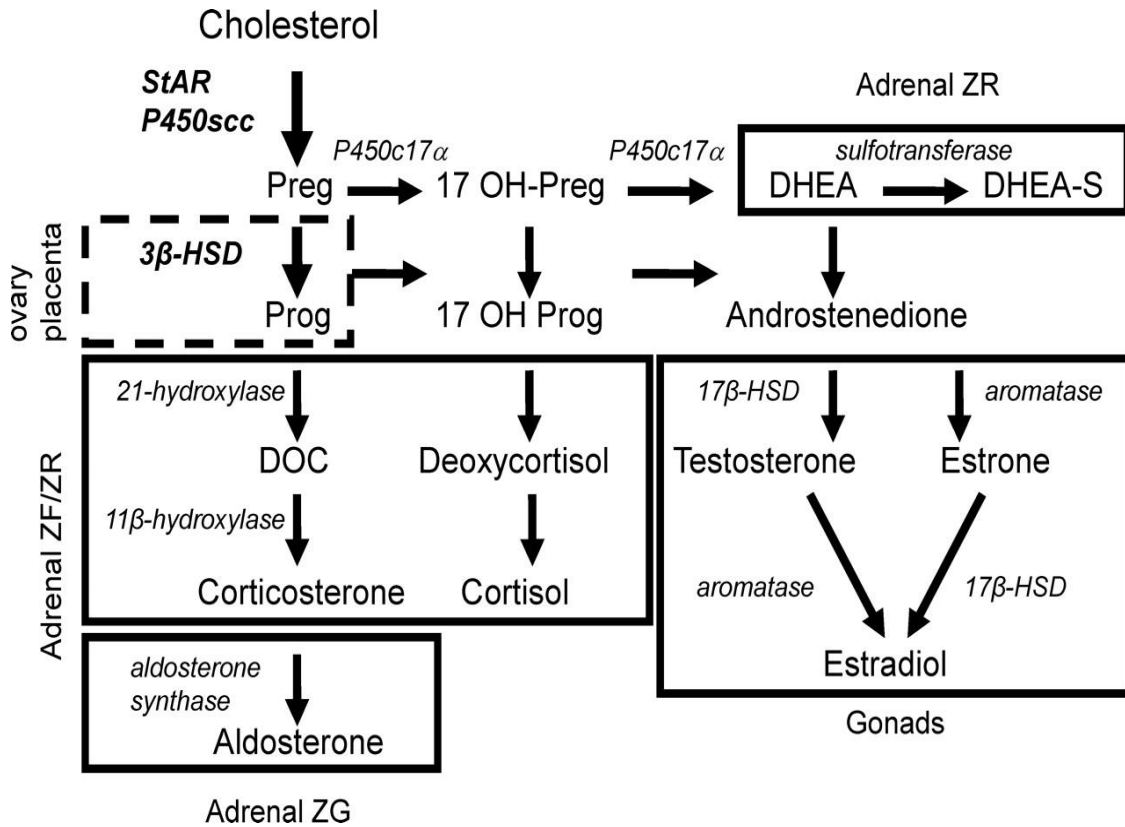


**Figure 1.2. Steroidogenic pathway.** Cholesterol is transported from the outer mitochondrial membrane to the inner mitochondrial membrane in theca cells and luteal cells by steroidogenic acute regulatory protein (StAR). Substrates are converted by their specific enzymes to the next substrate in the steroidogenic pathway (LaVoie and King 2009). Reused with permission.

START domain proteins bind sterols. START domain proteins are believed to control lipid trafficking between intracellular organelles, lipid metabolism, and signaling regulation (Soccio et al. 2005; Strauss et al. 2003). In humans, fifteen proteins with START domains have been identified. The START domain resides almost exclusively at C-terminals. They are sub-defined into six subfamilies, according to their sequence homology. Each subfamily is specialized in transporting and/or sensing of a common lipid ligand; for example, StAR (STARD1) and STARD3 share the ability to transport cholesterol. The STARD4 subfamily proteins (STARD4, STARD5, and STARD6) having greatest similarity to StAR, where they bind and/or transport cholesterol. While STARD2, STARD7, STARD10, and STARD11 proteins sense glycerolipid and sphingolipid and STARD13 senses phosphatidylcholine. The lipid-binding characteristics of the remaining START domain proteins have been less well characterized. However, the same sub-family members are distinct in their expression and subcellular localization; hence, their biological and physiological functions are different (Alpy and Tomasetto 2005; Alpy and Tomasetto 2014).

StAR is the founding member of the START domain protein family. Stocco and his team were the first to isolate the gene and describe for the 30 kDa mitochondrial StAR protein in MA-10 mouse Leydig tumor cells. They purified StAR protein performed mass spec sequencing and cloned a cDNA of 852 base pairs in length, which encoded a protein with 284 amino acids (Clark et al. 1994; Stocco and Clark 1996). StAR is mitochondria-targeting protein, and possesses a mitochondrial-signaling sequence at the N-terminus. StAR transfers cholesterol from the outer mitochondrial membrane into the inner-mitochondria membrane by its C-terminus. Steroidogenic efficiency is

determined by non-vesicular transferring of cholesterol by StAR into mitochondria, which is considered to be the rate-limiting and most regulated step in steroidogenesis in the adrenal and gonads. StAR gene expression is induced by ACTH and LH hormones via an increase in cAMP level in their target tissues. The increase in cAMP activates protein kinase A (PKA) and amplifies protein synthesis, phosphorylation events, and lipid synthesis leading to increased steroidogenesis (Rone et al. 2009; Soccio and Breslow 2004).

StAR synthesis and activity has been shown to be regulated by both PKA and protein kinase C (PKC) in a cell specific manner. In Leydig cell lines, MA-10 and TC-1, stimulation of PKC via phorbol-12-myristate-13-acetate (PMA) increased the total expression of StAR, but did not increase phospho-StAR its active form (P-StAR), and thus was unable to increase steroid production. However, combined stimulation of PKA with a sub-maximal dose of dibutyryl cAMP, leads to phosphorylation of StAR and increased steroidogenic activity. This finding indicates the importance of cAMP/PKA pathway in regulating steroidogenesis (Jo et al. 2005; Stocco et al. 2005). In addition, cAMP activates other transcription factors that modulate genes involved in steroidogenesis including StAR gene. These factors include as steroidogenic factor 1(SF-1), GATA-4, CREB, CCAAT/enhancer-binding protein (C/EBP), and SP1. Their binding sites are found in the 5'-flanking DNA proximal to StAR gene. Notably, the StAR promoter lacks a consensus cAMP response-element (CRE) often found in cAMP-responsive genes (Stocco et al. 2001; Tremblay et al. 2002; Manna et al. 2003).

Steroidogenesis can be activated by cAMP-independent pathways as well, such as growth factors, steroidogenic inducing protein, and calcium messenger signaling;

however, the other pathways have modest stimulation when compared to the cAMP/PKA pathway (Stocco et al. 2005). For example, insulin-like growth factors I and II (IGF-I and II) increased StAR protein expression approximately 4–5-fold (Soccio et al. 2005; Strauss et al. 2003). Furthermore, insulin increased StAR production by 2.5-fold in human luteinized granulosa cells. Production of progesterone parallels StAR levels in the same way in ovarian steroidogenic cells (Devoto et al. 1999).

### **1.7 STARD4 regulation**

Members of the STARD4 subfamily, STARD4, STARD5, and STARD6 have a START domain, and each domain consists of 205 to 233 amino acid residues. There is approximately 30% homology between STARD4 subfamily members. Structurally, the STARD4 subfamily is characterized by helix-grip fold from  $\beta$ -sheets and  $\alpha$ -helices. Internally, a deep pocket is formed by the curved  $\beta$ -sheet with C-terminal of the  $\alpha$ -helix, which produces an internal hydrophobic cavity, or a tunnel. Recently, x-ray structure of mouse STARD4 protein has been identified, and the estimation for the volume of lipid-binding tunnel was made at 847 Å resolution. It was found that the tunnel is able to accommodate one molecule of cholesterol (Romanowski et al. 2002; Soccio and Breslow 2003).

STARD4 was identified first in the mouse liver during analysis of cDNA microarray data of cholesterol-regulated genes (Soccio et al. 2002). The members of STARD4 subfamily are predicted to be close to StAR in their ability to transport cholesterol. In contrast to StAR, STARD4 and STARD6 lack an N-terminal mitochondrial targeting sequence. Targeting sequences are used to target the protein to specific organelle's membrane, which suggests cytoplasmic activity for both STARD4

and STARD6 although this has not been verified (Soccio et al. 2002). In the human, STARD4 has been identified in hepatocytes, Kupffer cells (liver macrophages in the parenchymal area), and THP-1 macrophages. At the subcellular level of these cells, STARD4 has been identified in the cytoplasm associated with ER and lipid droplets. It has also been co-localized with Acyl-CoA cholesterol acyltransferase-1 in ER-derived vesicles (Rodriguez-Agudo et al. 2011; Romanowski et al. 2002; Calderon-Dominguez et al. 2014).

Evidence in hepatocytes indicates that STARD4 is a cytoplasmic protein, which can act as non-vesicular transporter of cholesterol between the endoplasmic reticulum and the plasma membrane. The STARD4 gene is sterol-regulated, where its expression is reduced in the liver of mice fed a high cholesterol diet. STARD4 expression is controlled by the transcription factor SREBP-2, where it binds to sterol regulatory elements (SREs) on the STARD4 proximal promoter (Soccio et al. 2005; Alpy and Tomasetto 2014). Low levels of endoplasmic reticulum cholesterol activate SREBP-2, which upregulates the genes that are responsible for increasing cholesterol synthesis, uptake, and transport such as HMG-CoA reductase, LDL receptor, and STARD4, respectively (Goldstein et al. 2006). Overexpression of STARD4 increased the level of cholesterol in endoplasmic reticulum in mouse hepatocyte (Rodriguez-Agudo et al. 2008), where cholesterol gets esterified by ACAT; then esterified-cholesterol is stored in lipid droplets. Moreover, recombinant STARD4 has been shown to increase ACAT-1 activity, indicating that STARD4 participates in cholesterol esterification (Rodriguez-Agudo et al. 2011). Additionally, overexpression of STARD4 is increased nuclear liver X receptor (LXR) activity, which is involved in cholesterol metabolism. However, downregulation of

STARD4 by siRNA reduces the cholesterol level in endoplasmic reticulum and increases free cholesterol (Alpy and Tomasetto 2014; Miller 2007; Soccio et al. 2005) It was found that overexpression of STARD4 in STARD4-silenced cells enhanced the transport of sterol to the endocytic recycling compartment and to the endoplasmic reticulum (Mesmin et al. 2011). Conversely, only mild changes have been observed for lipid metabolism in STARD4 knock-out mouse. In Leydig cells, STARD4 expression was not induced by steroidogenic stimuli (Calderon-Dominguez et al. 2014; Riegelhaupt et al. 2010; Soccio et al. 2005). Nevertheless, recently the STARD4 subfamily (e.g., STARD4 and STARD6) has been shown experimentally to increase steroidogenesis in *in vitro* assays and in model cells, indicating STARD4 and STARD6 have the ability for cholesterol transport to the mitochondria (LaVoie et al. 2014; Bose et al. 2008). Additionally, non-steroidogenic COS-1 cells transfected with STARD4, the P450<sub>scc</sub> complex, and 3 $\beta$ -hydroxysteroid reductase revealed StAR-like activity of STARD4 as STARD4 was able to generate progesterone in this assay (Soccio et al. 2005).

### **1.8 STARD4 gene**

The human STARD4 gene is located on chromosome five (5q22.1), and it has six exons spanning 2.2 kb. The exon length of homo sapiens STARD4 in order are 75 bp, 113 bp, 49 bp, 126 bp, 114 bp, and 1,783 bp. Translation of STARD4 exons produces a wildtype protein of 200-205 amino acids. (Alpy and Tomasetto 2005; NCBI 2014 [http://www.ncbi.nlm.nih.gov/nucore/NM\\_139164.1](http://www.ncbi.nlm.nih.gov/nucore/NM_139164.1)). The STARD4 gene is classified in NCBI's Conserved Domain Database as a part of the SRPBCC ligand-binding domain superfamily. Domains have a deep hydrophobic ligand-binding pocket and bind for a different ligands as mentioned above (Marchler et al. 2015). Upregulation of STARD4

causes an increase in the level of cholesterol in the endoplasmic reticulum and cholesterol esterification (Soccio et al. 2005). Cholesterol trafficking between the endoplasmic reticulum, endocytic recycling compartment, and plasma membrane were disrupted in HepG2 cells when STARD4 expression was knocked down, which indicates STARD4 plays a role in cholesterol transport by the non-vesicular pathway (Garbarino et al. 2012).

### **1.9 STARD6 protein**

STARD6 is one member of STARD4 subfamily, which is characterized by binding cholesterol and oxysterol. Structurally, STARD6 is similar to STARD1 with unique C-terminus, which is sensitive to protease. STARD6 was first identified in male germ cells, which led to the hypothesis that the protein participates in spermatogenesis rather than steroidogenesis (Clark 2012; Gomes et al. 2005). However, STARD6 was later localized in Leydig cells and in various nervous tissues inferring a possible role in steroidogenesis. STARD6 was localized in the cytoplasm and nucleus of these cells (Chang et al. 2010). Recently, STARD6 has been detected in the luteinizing granulosa cells of the pig ovary, which have steroidogenic ability; however, the cAMP pathway did not regulate STARD6 (LaVoie et al. 2014). *In vitro* STARD6 efficiency in transporting cholesterol into adrenal mitochondria was equal to STARD1 (Bose et al. 2008). To date, almost nothing is known about the regulation of STARD6 at the gene or protein level.

### **1.10 Diseases related to START proteins and steroid production**

Only one disease has been proven to be related to one of the START proteins, which is Lipoid Congenital Adrenal Hyperplasia (CAH). Lipoid CAH is a fatal disease caused by mutation in StAR gene associated with the complete absence of steroidogenesis. The most organs affected are the adrenal gland and the testis. Initially,

the steroidogenic tissue can keep low level of steroidogenesis by StAR-independent pathway; however later cells are unable to produce any steroid hormones. The adrenal and testicular tissues lose their ability to convert the cholesterol to the pregnenolone; therefore, they are destroyed due to accumulation of cholesterol and cholesterol ester (Lin et al. 1995; Miller 1997; Miller and Bose 2011). The StAR knockout mouse has the same phenotype as human lipid CAH. Both the level of corticosterone and aldosterone are decreased with elevation of ACTH and CRH (corticotropin releasing hormone), indicating insufficient production of steroid hormones by the adrenal gland. StAR knockout mice prematurely die, as lipid deposits in the adrenal cortex cause disruption (Caron et al. 1997).

Diminished Ovarian Reserve (DOR) is a second most common cause of infertility at any age, where the ovaries lose their follicles for unknown reason. A study comparing DOR patients during IVF cycles and normal egg donors at a similar age, observed multiple differences in gene expression. The StAR and STARD4 genes were significantly increased in DOR patient luteinized granulosa cells by microarray analysis compared to those of normal patients (Skiadas et al. 2012).

Interestingly, there are association between STARD1 expression and non-alcoholic fatty liver diseases (NAFLD). There is an increase in the expression of STARD1 in patients with NAFLD. Simultaneously, hepatic free cholesterol was elevated and SREBP2 transcriptional factor with hydroxyl methyl glutaryl-CoA reductase liver enzyme were elevated too. Similar results were detected in a mouse model with NAFLD, where the accumulation of cholesterol led to development of non-alcoholic steatohepatitis (Clark 2012; Caballero et al. 2009; Rooyen et al. 2011). Additional studies investigated

mitochondrial cholesterol level in a human hepatocellular carcinoma, the human HepG2 hematoma cell line, and rat H35 cell line. All samples have shown elevation of cholesterol contents of hepatic mitochondria as a mechanism to resist the apoptosis-inducing agents; additionally, SREBP2 and STARD1 were overexpressed (Montero et al. 2008; Clark 2012).

### **1.11 Aims of this study**

STARD4 and STARD6 have recently been identified in granulosa cells, however, only two published studies have examined their expression and possible function in the ovary (Skiadas et al. 2012; LaVoie et al. 2014). Our laboratory also has found STARD4 and STARD6 mRNA and protein in human luteinized granulosa cell preparations by PCR and Western blot, respectively. To understand the function of STARD4 and STARD6 in the ovary and whether these molecules can contribute to the steroidogenic ability of ovarian cells, we need to first have some basic descriptive information regarding these proteins in the ovary. My research is mainly focused on localization and expression of STARD4 and STARD6 in human ovarian tissue and luteinized granulosa cells.

#### **Specific Aim 1:**

To determine the presence and expression of STARD4 and STARD6 mRNA and proteins in available human ovarian tissues by real-time PCR and Western blot.

#### **Specific Aim 2:**

To localize STARD4 and STARD6 proteins in different sections of human ovarian tissues by using immunohistochemistry.

**Specific Aim 3:**

To determine the subcellular localization of STARD4 in primary human granulosa cells by confocal microscopy.

**Specific Aim 4:**

To determine and clone the major STARD4 mRNA transcript(s) in human luteinized granulosa cells.

**Specific Aim 5:**

To compare the size of recombinant human STARD4 protein(s) generated from the granulosa cell transcript(s) isolated in Aim 4 with endogenous STARD4 protein from human ovarian tissues and granulosa cells by Western blot and to test the steroidogenic ability of the resulting recombinant proteins in COS cells expressing the P450<sub>scc</sub> complex.

## Chapter II

### Materials and Methods

#### **2.1 Human granulosa cell isolation**

Human follicular fluid including residual granulosa cells was harvested from women undergoing reproductive assisted techniques at the Advanced Fertility and Reproductive Endocrinology Institute, West Columbia, SC. The follicular fluid was transported on ice as soon as possible to the LaVoie lab at the University of South Carolina, School of Medicine. All cell isolation and culture procedures were performed in a laminar flow hood under sterile conditions. The follicular fluid for each patient was kept separate and was transferred into one or more 50 cc tubes, and spun at 2000 rpm in a Beckman TJ-6 refrigerated centrifuge for 20 minutes. The supernatant, which was comprised of follicular fluid and any contaminating sera, was poured off. Pellets which contained blood cells and luteinized granulosa cells, were resuspended in 3 ml of 2X enzyme mixture of Hyaluronidase (100 mg/ml, Sigma, St. Louis, Mo) and DNase (6.25 mg/ml, Sigma), which were dissolved in DMEM/F12 media. The resuspended pellets were incubated in the culture incubator for 10 minutes to dissolve granulosa cells connections. During the incubation, a discontinuous Percoll (GE Healthcare) gradient was prepared for each pellet in a 15 cc tube by adding 4 ml of 70% Percoll in PBS at the bottom and overlaying 4 ml of 35% Percoll in DMEM/F12 media with antibiotics on top. The cell-enzyme mixture was added gently onto the upper Percoll layer and spun at 2000 rpm for 30 minutes to partition cells and pellet contaminating blood cells.

Individual granulosa cells and granulosa cell clusters formed one to two low density bands. Both bands were collected and for each patient's cells were pooled and placed in new tube. The collected sample was brought up to 22-25 ml by adding DMEM/F12 plus antibiotics and filtered through 70  $\mu\text{m}$  cell strainer into clean 50 cc tube to remove any large granulosa cell clumps. The cells were spun again at 2000 rpm for 20 minutes to pellet. After the supernatant was removed, the cell pellet was suspended in 300 to 800  $\mu\text{l}$  of DMEM/F12 containing antibiotics and the total volume was measured for the purposes of calculating total cell number. For counting, 10  $\mu\text{l}$  of cell suspension was added to 1000  $\mu\text{l}$  of DMEM/F12 + ab medium followed by the addition of 100  $\mu\text{l}$  of trypan blue dye. The cells were plated in 12 well Falcon plates approximately at  $2-4 \times 10^5$  live cells per well in 1 ml of complete human granulosa cell media (DMEM/F12 + 1X antibiotic antimycotic solution, 50  $\mu\text{g/ml}$  gentamicin, and 10% fetal bovine serum (FBS)). Cells were cultured at 37  $^{\circ}\text{C}$  with 5%  $\text{CO}_2$  in humidified cell culture incubator. The media were changed daily every 24 hours for 3 days after plating. Some of the plates were treated, and some were not treated for confocal staining.

## **2.2 Protein isolation**

Whole cell extract (WCE) buffer was used to lyse hGC and COS cells for protein isolation. WCE buffer is composed of 50 mM Tris (pH 7.5), 1% NP-40, 0.5% sodium deoxycholate, 0.1% sodium dodecyl sulfate (SDS), 150 mM NaCl, 1 mM EDTA, 0.3% ALLN, 1% Pierce protease inhibitor cocktail, 1% Pierce phosphatase inhibitor, and sterile water. For the COS F2 steroidogenic assay (detailed below) 1 ml of media from each well of COS cells was collected and stored at -80  $^{\circ}\text{C}$  for pregnenolone quantification later. The rest of the media was aspirated off cells and the hGCs and COS cells were rinsed

with 1-2 ml of Dulbecco's phosphate buffer saline (D-PBS) at room temperature. After removing PBS, ice cold WCE buffer was added to each well (100  $\mu$ l for hGC, 150  $\mu$ l for COS cells). The cells were gently scraped by rubber scraper and transferred to 1.5 ml microfuge tube. The cells were incubated with lysis buffer on ice for 30 minutes. The mixture lysate was spun at 13,000 rpm in a microcentrifuge (Eppendorf centrifuge 5417R) for 15 minutes at 4 °C. The supernatant was transferred into new labeled tube, and then the volume was measured for the purpose of calculating total protein when protein assays were performed later. The tube was stored at -80 °C.

### **2.3 Protein quantification**

Quantification of protein was performed by method of Bradford using Bio-Rad protein dye reagent and a spectrophotometer set at 595 nm. A standard curve was generated using known concentrations of bovine serum albumin protein (BSA, 0-8 mg/ml), then the protein quantities were extrapolated from the linear region of the standard curve. The samples of the protein were diluted (30-50  $\mu$ g) and aliquoted for SDS-PAGE and Western blotting.

### **2.4 SDS-polyacrylamide gel electrophoresis and immunoblotting**

The samples with same amount of protein were mixed with 5X bromophenol blue loading dye containing 5% 2-mercaptoethanol on ice. Precast 4-20% acrylamide gels (Pierce, ThermoScientific) were used with a Bio-Rad minigel apparatus for protein separation. Gel running buffer was added (80 ml of 10X running buffer and 720 ml nanopure water). The 10X running buffer was made by adding 57.3 g glycine, 12.1 g Trizma Base, and 4 g SDS, and filled up to 500 ml with nanopure water. Wells were flushed prior to loading. The protein samples were heated at 100 °C for 8 minutes prior to

loading, were spun briefly and then entire sample was loaded into the well. The gel was run at 200 V for 45 min to 1 h. Protein in gels was transferred to Hybond-P PVDF membrane by semi-dry electroblotting (Owl Panther semi-dry electroblotter). Transfer buffer was composed of 2.93 g glycine, 5.82 g Trizma Base, and 200 ml methanol, and filled up to 1 liter with nanopure water. After wetting the membrane briefly in methanol, the transfer stack was prepared layering three sheets of pre-cut, pre-wet (in the transfer buffer) Whatman paper, the gel, the PDVF membrane, and three additional sheets of Whatman paper. The transfer occurred under environments of constant current, starting at a voltage of 9-10 for 90 minutes.

## **2.5 Western blot**

The membrane was blocked in 5% nonfat dry milk (Carnation)/1X Tris buffered saline with Tween (TTBS) for 1 hour or 2 hour (post-stripping). TTBS (1X) contained 100 ml 10X TBS, 900 ml nanopure water and 0.5 ml Tween-20 per liter. 10X TBS, pH 7.5 was composed from 24.2 g Trizma Base, 292 g NaCl, and filled up to 1 liter with nanopure water. After blocking, the membrane was washed with 1X TTBS for 3 times, 10 minutes each. The membrane was placed in a small container to apply primary antibody. The antibodies used were against STARD1 (1:1500); this antibody was gift from Dr. Steven King and Dr. Douglas Stocco (Texas Tech University, Health Sciences Center). STARD4 (1: 200, 0.5 µg/ml, Abgent, Atlanta, GA, Cat. # AP12801a, Lot # SA110414AR,), STARD6 (2.5 µg/ml, Abgent, Cat. # AP11832b, Lot # SA 110210AB) and CYP11A1 (0.5 µg/ml, Abgent, Cat. # AP7899a, Lot # SH081229L (Atlanta, GA). The actin antibody (1:500, Cat. # 4967, Lot # 6) was obtained from Cell Signaling, Danvers, MA. The primary antibodies was diluted in 1% nonfat dry milk/1X TTBS, and

applied to the membrane, with the exceptions of STARD1 antibody was diluted in 5% milk. Approximately 3 ml of antibody solution was used onto each membrane. Membranes were incubated with antibodies at 4 °C overnight on a shaker. The secondary antibody was pre-absorbed overnight at 4 °C by mixing 2 µl of Goat anti-rabbit secondary antibody (Zymed, Cat. # 65-6120, Invitrogen/Life Technologies), 2 µl BSA (2µg), and 96 µl PBS. The following day, the membrane was washed with 1X TTBS for 10 minutes, 3 times. The pre-absorbed secondary antibody was diluted in 5% nonfat dry milk/1X TTBS to a final concentration of 1:5000 and applied on the membrane and shaken for 1 hour at room temperature. Afterwards, the membrane was washed with 1X TTBS 5 times, 10 minutes each. ECL (ThermoScientific) solution was prepared immediately before it was used by adding 1:1 of Reagent 1 to Reagent 2 of the ECL kit. The ECL solution was added onto well-drained membrane for 1 minute. The membrane was drained well, and then the membrane was placed inside a film cassette between two pieces of transparency plastic. A spectrum of timed film exposures in the dark room was performed and developed (Classic X-ray Film/ Research products International Corp). After exposure, the membrane was washed with 1X TTBS for 5 minutes, 3 times each to prepare for stripping.

## **2.6 Stripping immunoblots**

The stripping buffer (50 ml) was made up of 6.25 ml 0.5 M Tris-Cl (pH 6.8), 10 ml 10% SDS, 0.35 ml 2-mercaptoethanol, and 33.4 ml nanopure water. The membrane was washed 3 times, 5 minutes each with 1X TTBS. The 1X TTBS was poured off and approximately 50 ml of erasing buffer was added to each membrane. The membrane was placed in a hybridization oven preheated at 60 °C with agitation for 45 minutes. The

erasing buffer was poured off, and the membrane was washed 4-5 times in 1X TTBS for 10-15 minutes each over the course of an hour. The membrane was blocked for 2 hours before applying another primary antibody.

## **2.7 RNA Isolation and cDNA Synthesis**

RNA was isolated from human ovarian tissues. The frozen luteal tissues were obtained from the Cooperative Human Tissue Network (University of Alabama) and the two follicular phase ovarian biopsy samples were collected by Dr. LaVoie in cooperation with the Dept. of Obstetrics and Gynecology. All work with human tissues was reviewed and approved by the University of South Carolina Institutional Review Board. The tissue biopsies were placed on dry ice until the lysis buffer was added. Trizol (500  $\mu$ l) was added to each sample, then tissue samples were homogenized with 10 strokes of a Dounce homogenizer to shear the tissue. The sample was transferred to RNase-free microfuge tube and incubated for 5-10 minutes at room temperature. Then, the samples were centrifuged for 1 minute at 12,000 xg at 4 °C to pellet non-soluble tissue and only the supernatant of each sample was pipetted and transferred into new RNase-free tube. An equal volume of 95-100% ethanol was added and mixed thoroughly. Each lysate sample was loaded into Zymo-Spin column (Directzol Kit, Zymo Research) and centrifuged for 1 minute at 15000 xg in a microfuge at 4 °C. RNA Wash buffer (400  $\mu$ l) was added into each column and centrifuged for 1 minute. DNase cocktail (80  $\mu$ l) was added to each column and incubated for 15-20 minutes at room temperature then centrifuged for 30 seconds. The DNase cocktail was prepared immediately before it used according to kit instructions. RNA Prewash buffer (400  $\mu$ l) was added into each column and centrifuged for 1 minute. After repeating the previous step, 700  $\mu$ l of RNA Wash

buffer was added into each column and centrifuged for 1 minute. The columns were centrifuged for 2 minutes more to dry the columns. The flow-through was discarded in all previous steps. The RNA was eluted from the column by adding 40  $\mu$ l of RNase-free water, incubating 5 min at room temperature, and collecting the fluid in new collecting tubes by centrifuging for 2 minutes. The RNA concentrations were assessed by spectrophotometer at wavelength of 260 nm, then diluted for cDNA synthesis. The samples were kept on ice for use or stored at - 80°C.

The diluted RNA samples were reverse transcribed into cDNA using Bio-Rad iScript cDNA synthesis kit. The reaction assembled by adding 15  $\mu$ l of RNA sample (400 ng), 4  $\mu$ l of 5X iScript reaction buffer, and 1  $\mu$ l of iScript Reverse Transcriptase enzyme. The tubes were incubated for 2 minutes at room temperature, then the reaction was carried out in a thermal cycler for 5 minutes at 25 °C, 30 minutes at 42 °C, and 5 minutes at 85 °C, and held at 4 °C or placed on ice. Each sample of cDNA was diluted with DNase/RNase-free water to concentration of 10 ng/ $\mu$ l. The cDNA either were kept on ice to use for a real time PCR or stored at -20 °C.

## **2.8 Real-time PCR**

To quantify the amount of STARD4 and STARD6 transcripts in different ovarian tissues, real-time PCR was used. The cDNA samples were amplified in duplicate or triplicate by using the iCycler Real-Time PCR Detection system (Bio-Rad). A water negative control was included in each PCR run. Each PCR reaction was composed of 0.2-1.0 ng/ $\mu$ l cDNA, 2X SsoAdvanced SYBR Green Supermix (Bio-Rad), upstream primer, and the same amount of downstream primer with concentrations of 600 nM for hSTARD4, and 300 nM for hSTARD6, and PCR-grade water to bring the volume to 20

µl. The PCR upstream primer for hSTARD4 was 5'-CAAAGCCCAAGGTGTTATAGATGAC-3' and the downstream primer was 5'-ACAGCAATTCTCTTCAAAGTTCTCC-3'. The PCR upstream primer for hSTARD6 was 5'-TTCATATGTCATACCATTACACAAAG-3' and downstream primer was 5'-CTCATTTCTGTCTGGACAAACATCAC-3'. The real-time PCR was performed with initial denaturation at 95 °C for 2.5 min followed by 40 cycles for hSTARD4 or 45 cycles for hSTARD6 of denaturation for 15 seconds at 95 °C, annealing for 30 seconds at 62 °C (hSTARD4) or at 60 °C (hSTARD6), elongation for 30 seconds at 72 °C. A ten minute final extension at 72 °C was performed. A single product was confirmed by the presence of a single melting curve peak and the average threshold cycle (Ct value) was used to quantify the results. Human TATA-box binding protein (hTBP) was used as an internal amplification control as our lab has found this mRNA to be constitutively expressed. The PCR primers for hTBP generated an 87-bp amplicon and were derived from GenBank. The upstream primer was 5'-CACGGCACTGATTTTCAGTTC-3' and the downstream primer was 5'-TCTTGCTGCCAGTCTGGACT-3' with concentration of 312.5 nM/ 20 µl reaction. All amplicons derived from these primers sets have been previously sequenced to confirm the amplicon identity and characterized by others in the laboratory. Target mRNA starting quantity was performed by the standard curve method. A standard curve was generated for each amplicon by serial diluting a known amount of purified amplicon, determining the Ct value for each starting amplicon concentration. Ct values for tissue were extrapolated from a linear plot of log concentration and Ct values. The quantity of STARD4 or STARD6 in each tissue was normalized to its corresponding quantity of hTBP.

## **2.9 Immunofluorescent labeling of STARD4 for confocal imaging**

The hGC and COS-1 cells were fixed in 2% paraformaldehyde and stored at 4°C until use. Coverslips were placed in a fresh 6-well cell culture plate for staining. The cells were incubated with 1 ml of PBS/ 0.01Glycine/ 0.1% Triton-X per well for 15 minutes, 3 times. The cells were incubated with 5% IgG-free BSA/PBS for 10 minutes. One ml of normal donkey serum (5 %), which dissolved in 1% BSA/PBS, was used as blocking solution for 10 minutes. Each well of the cells were incubated with 1 ml of primary antibody, which was diluted in 1% BSA/PBS, for 1 hour at 37 °C. The primary antibodies included STARD4 Abgent rabbit antibody at a concentration 1:100 (Cat # AP12801a; Lot # SA110414AR), and Glucose-regulated protein 78 (GRP78) Lot # J2214; Santa Cruz goat polyclonal antibody at a concentration 1:20. The coverslips were washed with 1.5 ml of 1% BSA/PBS twice for 15 minutes, then incubated with 1 ml of 5% normal donkey serum per well for 10 minutes. The plates were covered with foil in all subsequent steps. The cells were incubated with 1 ml of secondary fluorescent antibody per well (diluted in 1 % BSA/PBS) for one hour at 37 °C. The secondary antibody included donkey anti-rabbit (DAR-IgG, Cy3) antibody with concentration of 1:100 (Code # 711-165-152; Lot # 118786) and donkey anti-goat (DAG-IgG, Cy2) antibody with concentration of 1:100 (Code # 705-225-003; Lot # 90026). Both secondary antibodies obtained from Jackson ImmunoResearch, USA. The cells were washed with 1 ml of 1% BSA/PBS per well for 15 minutes two times, and the third wash with 1.5 ml of PBS for 15 minutes. For double-labeling, the cells were incubated with STARD4 primary antibody and Cy3 secondary antibody first, then after washing, we repeated the procedure for the GRP 78 primary antibody and Cy2 secondary antibody. To

visualize the nucleus, the cells were incubated with 1 ml of 5 mg/ml 4',6-diamidino-2-phenylindole dihydrochloride (DAPI) per well for 15 minutes. The plates were washed with 1.5 ml of PBS for 15 minutes twice. Most of the incubation and washing steps were done on the shaker, except the primary and secondary antibodies incubations. The coverslips were mounted with one drop of DABCO in the middle of the slide, and slowly pulled down the coverslips on the slide to avoid bubbles.

### **2.10 Confocal imaging**

A Zeiss LSM 510 META Confocal Laser Microscope was used to image the slides. The excitation/emission wavelengths for DAPI complexes was 358 nm/461 nm. The excitation/emission wavelengths for Cy3 complexes was 550 nm/570 nm. The excitation/emission wavelengths for Cy2 complexes was 492 nm/510 nm.

### **2.11 Immunohistochemistry**

Paraffin-embedded sections of human ovarian tissues with thickness of 5-8  $\mu\text{m}$  were placed on poly-lysine coated microscope slides. The sections were deparaffinized by xylene and rehydrated by series of ethanol washes, then rinsed with tap water. Antigen retrieval procedure was performed to unmask the antigen sites (Gillio et al. 2003). The sections were immersed in 0.01 M citrate buffer solution with pH 6.0, then they were heated by microwave in microwave pressure cooker for 20 minutes at 800 W followed by 15 minutes at 300 W. Slides were allowed to cool for 10-15 minutes then rinsed with water for 5 minutes followed by washing in D-PBS for 10 minutes. Endogenous peroxidase activity was blocked by incubating the slides in the 0.3% peroxide mixed with methanol for 40 minutes. Slides were washed by D-PBS for 10 minutes. Sections were incubated for an hour in the blocking solution of 10% goat serum-PBS. An initial dilution

series of each primary antibodies was tested to determine the optimal concentration for IHC. To localize human STARD4 and human STARD6 proteins, the human ovarian tissue sections were incubated in 200  $\mu$ l of STARD4 (1:100, Abgent, Cat # AP12801a; Lot # SA110414AR), or STARD6 (1:100, Abgent, Cat. # AP11832b, Lot # SA 110210AB) primary rabbit antibodies overnight at 4 °C. The negative control slides were incubated in blocking solution only. After washing with D-PBS, the tissue sections were incubated in 200  $\mu$ l of goat anti-rabbit (GAR) secondary antibodies with concentration of 1:600.

To visualize bounded antibodies, the slides were incubated with 3,3-diaminobenzidine (DAB) solution for exactly 3 minutes at room temperature then washed in tap water. Subsequently, the sections were incubated for 15 seconds in 100% hematoxylin solution to counterstain the tissues, then washed in tap water for 10 minutes. The slides were dehydrated by series of ethanol washes and xylene. Positive staining was present as a brown color. The specificity of immunohistochemistry signal was determined by performing preabsorption studies with the respective blocking peptides for STARD4 or STARD6 primary antibodies. Primary antibodies were incubated overnight at 4 °C with or without 200-fold molar excess of its target peptide (Abgent) prior to use. The sections were examined with 10, 20, 40, and 63x objectives using a Zeiss microscope (Carl Zeiss MicroImaging, Inc., Thornwood, NY). Images were captured using a SPOT camera and software (Diagnostic Systems Inc., Sterling Heights, MI). Final images were generated using Photoshop.

## **2.12 Cloning of human STARD4 transcripts**

Pooled cultured human granulosa cells from multiple patients was used to make poly (A) RNA. Human granulosa cells total RNA (91.7 µg) was utilized as starting material with the MicroPoly (A) Purist Kit according to the manufacturer's instructions (Ambion). After precipitating the RNA sample, the resuspended RNA pellet was bound to Oligo (dT) cellulose. The recovered volume of poly (A) RNA was 10 µl with concentration of 126 ng/µl. The hGC cDNA library was made from poly (A) RNA using the Clontech Marathon cDNA Amplification Kit (Takara Bio Company, USA) with starting amount approximately 0.630 µg of poly (A) RNA. Human placental poly (A) RNA (1 µg), provided with the kit, was run at the same time as a positive control. The first and second strands of cDNA were synthesized according to the kit instructions. After the second-strand was made, an aliquot of the sample was ligated to Marathon cDNA Adaptors. Two dilutions, 1:50 and 1:250, were prepared for the hGC and placental adaptor-ligated double-stranded cDNA libraries to perform the nested 5' and 3' RACE-PCR reactions.

The hGC adaptor-ligated cDNA (1:250) mixed with either hSTARD4-nested-3' RACE-US (5'-CATAGCATTGAAGAAGATAAGTGGCGAGTTGC-3'), or hSTARD4-nested-5' RACE-DS (5'-ATGGCTGTATCTACCGCAGACTGAGGAATC-3'), and Adaptor primer 1 for the first outer reaction of 25 cycles at annealing temperature of 68 °C, melting temperature of 94 °C, and 72 °C for extension. The PCR products of the first reaction was diluted by adding 245 µl of Tricine EDTA buffer to 5 µl from the first reaction. For the second nested reaction, the diluted product was added to either hSTARD4-3-RACEex4-US (5'-AGGGCCTTGTCGTTTGGATTGGGACAGCTTG) or

hSTARD4-5-RACEex4-DS (5'-CAAGCTGTCCCAATCCAAACGACAAGGCCCT), and adaptor primer 2 for 20 cycles with annealing temperature at 68 °C. The PCR products were cloned into PCRII vector (4.0 kb) by TA cloning, then transformed into TOP 10 One Shot competent E. coli cells and plated on LB-agar plates containing ampicillin (50 µg/ml) and grown overnight. X-Gal was used to differentiate between the colonies with plasmid inserts and those without. The brightest white colonies were cultured in liquid Lennox Broth base media (LB Broth, Life Technology) with ampicillin overnight at 37 °C in the shaker incubator. Plasmids were purified using the QIAprep Spin Miniprep Kit. Minipreped plasmids were screened for inserts by EcoRI restriction enzyme digest and run on 1.2% agarose gels. The positive plasmid products were sent to Genewiz Company for sequencing. The sequence results were analyzed by BLAST, and they found to match Homo sapiens StAR-related lipid transfer domain containing 4, mRNA, and variants X1, X4, and X5 transcripts at GenBank, NCBI website.

The different transcripts were aligned with the predicted wildtype STARD4 mRNA in order to design primers for full length transcripts. Primers were designed to the conserved 5'-UTR and near the stop codon to try to amplify the wildtype and full-length variants. The upstream primer was hSTARD4FL-US (5'-CTTCCACGTCCTTGCTTCA CCTCAG) and the downstream primer was hSTARD4FL-DS (5'-GCCATGTAGCTGA GAGAGTTGATCTG). Full length hSTARD4 transcripts were amplified by PCR using hGC Marathon cDNA library without adaptors, hSTARD4FL upstream and downstream primers with Advantage 2 polymerase and 10X Advantage 2 PCR buffer for 35 cycles; under the condition of 94 °C melting temperature for 15 seconds, Annealing temperature at 65 °C for 30 seconds, and extension temperature at 72 °C for 2 minutes. PCR products

were gel purified from 1.2 % agarose gels and cloned into the PCR2.1-TOPO vector and transformed into TOP 10 One Shot competent *E. coli* cells. The brightest white colonies was cultured in liquid LB Broth media with ampicillin as mentioned above, then the plasmids DNA purified by QIAprep Spin Miniprep Kit and screened by EcoRI digest. The positive plasmid products were sent to Genewiz Company for sequencing. The resulting sequences were matched again to *Homo sapiens* StAR-related lipid transfer domain containing 4, mRNA, and their variants transcripts at GenBank. The clones corresponded to the predicted STARD4 wildtype and one variant with an exon 4 deletion. The exon 4 deletion introduces a premature stop codon.

The positive inserts were excised using EcoRI enzyme from PCR2.1-TOPO vector and ligated into linearized pcDNA 3.1, an expression vector. The pcDNA3.1 vector was linearized by EcoRI enzyme and ends dephosphorylated with calf intestinal alkaline phosphatase according to the instructions of the manufacturer (Promega). The dephosphorylated pcDNA 3.1 was purified using the QIAquick PCR purification kit. The ligation reaction was done using T4 DNA ligase and 1:1, 1:3, or 3:1 molar ratios of vector:insert DNA. The reactions were incubated for 3 hours at room temperature and transformed into DH5 $\alpha$  competent *E. coli* cells. The overnight liquid cultures were purified by QIAprep Spin Miniprep Kit, and screened by EcoRI enzyme and agarose gels for the predicted sizes of the STARD4 inserts.

The positive pcDNA3.1 with STARD4 inserts were screened for forward and reverse orientation by EcoRV enzyme. The forward insert yielded a band of 535 bp, and the reverse orientation had a band size of 204 bp. The positive plasmids with forward orientation were sent into Genewiz Company for sequence and orientation confirmation.

Larger scaled plasmid preps for transfection were purified according to QIAGEN Plasmid Midi and Maxi Purification Kit.

### **2.13 COS-1 cells culture**

COS-1 cells were resurrected from frozen stock and incubated in a 10 cm culture dish with COS-1 complete media (DMEM/F12, 1X antibiotic antimycotic solution, 10% FBS) and split every 3-4 days. When the cells were at least 90% confluent, the cells were detached by adding 2 ml of Trypsin-EDTA solution and incubated in the incubator for 3-4 minutes with periodic dish shaking and microscopic inspection. When the cells were mostly detached, 4 ml of COS-1 complete media was added, and the whole solution was transferred to 50 cc tube. The cells were spun at 1200 rpm for 8 minute at 4 °C. After removing the supernatant, the cell pellet was resuspended in fresh COS-1 complete media. One 10 cm dish of near confluent cells was used to seed all the wells of a 6-well culture plate. Each well received 2 ml of media. For the COS-F2 assay below, 10 wells were plated.

### **2.14 COS-F2 steroidogenic assay**

To test the steroidogenic ability of full-length STARD4 and truncated STARD4 transcripts derived from human granulosa cells, the COS-F2 steroidogenic assay was utilized. COS-1 cells were split into 6-well culture dishes and cultured for two days before the experiment set-up. Cells were 60-80% confluent at the start of transfection. All plasmids were amplified in DH5 $\alpha$  bacteria and purified using the Qiagen Midi Prep kit. For each well, 2  $\mu$ g of plasmid DNA was prepared which included 1  $\mu$ g of pCMV-F2 plasmid (which makes a fusion protein with all components of the P450<sub>scc</sub> complex needed to make steroids), 10 ng of Renilla Luciferase plasmid (p-tkRL-Luc, a

transfection control), and equimolar amounts of pcDNA-hSTARD4 FL-6 (encodes wildtype STARD4) or pcDNA-hSTARD4 FL-13 (encodes truncated STARD4) or the backbone vector pcDNA3.1 (negative control). When necessary the pcDNA3.1 vector was used to normalize DNA to 2 µg. In addition, as a positive control to demonstrate the F2 plasmid was working, additional wells were transfected with pCMV-STARD1, which has consistently been shown to increase pregnenolone production in COS-1 cells in the presence of the F2 plasmid. All plasmids were diluted in antibiotic-free, serum-free DMEM/F12 and combined with Lipofectamine (8 µl/well, Invitrogen) diluted in similar media and incubated for 15-20 min to allow DNA-lipid complex formation. DMEM/F12 was added up to 1 ml total/well and the transfection mixture was overlaid onto rinsed COS-1 cells, which were incubated for 6 h. Cells were transfected in duplicate wells. The transfection mix was removed and transfected COS-1 cells received 2 ml of complete media. After a recovery period of 18-19 hours, the medium was replaced with 2 ml of fresh complete medium and incubated an additional 24 hours. At the end of the 24-hour period, 1 ml of the media was collected from each well and stored for Pregnenolone ELISA. One well of each duplicate was lysed with whole cell extract lysis buffer (described above) for Western blot. The second well was lysed with Passive lysis buffer (Promega) for luciferase assay.

### **2.15 Luciferase Assay**

COS cells were lysed in 1X Passive lysis buffer and stored at -80 °C. The samples were thawed and briefly mixed by vortex. The samples were spun down in microcentrifuge at 14,000 rpm for 2 minutes and then the supernatant was transferred to new labeled tube. Renilla luciferase activity was measured with reagents in the Dual-

luciferase assay kit. Twenty  $\mu\text{l}$  of sample was assayed with 100  $\mu\text{l}$  of Renilla luciferin substrate. Light production was measured with a Luminometer (TD-20/20 Turner Designs).

### **2.16 Pregnenolone ELISA assay**

Pregnenolone secretion into the media by COS-1 cells used in the F2 steroidogenic assay was measured by ELISA (Alpco). The samples were thawed and spun in the microcentrifuge at 14,000 rpm for 2 minutes to pellet cell debris and clarified supernatant was transferred to a clean tube. Wash buffer, biotin conjugate, and Horseradish Peroxidase conjugate solutions (HRP) were prepared before starting and kept a room temperature. Pregnenolone standards, high and low kit controls, and samples (50  $\mu\text{l}$ ) were pipetted into assay wells in duplicate. Biotin conjugate working solution (100  $\mu\text{l}$ ) was added into each well and the microwell plate was incubated on plate shaker for one hour at room temperature. The wells were washed 5 times with 300  $\mu\text{l}$  of diluted wash buffer per well and taped firmly against absorbent paper to ensure that all wells are empty. After aspiration of the final wash, the plate was incubated on a plate shaker for 30 minutes with 150  $\mu\text{l}$  of HRP conjugated working solution in each well. The plate was washed 5 times by 300  $\mu\text{l}$  of wash buffer per well. 150  $\mu\text{l}$  of TMB substrate was added into each well at timed intervals and incubated on the shaker for 10-15 minutes. After adding 50  $\mu\text{l}$  of stop solution into each well at timed intervals, the plate was scanned with a microwell plate reader (Benchmark plus, Bio-Rad laboratories) at 450 nm to get the optical density (OD) reading. Pregnenolone concentrations were extrapolated from a standard curve of log concentration and OD values. It was necessary to dilute some

samples 1:2, 1:5, or 1:10 before the assay to have their values fall in the reliable region of the standard curve. Pregnenolone concentrations were normalized to total protein in the well.

### **2.17 Data analysis**

We examined STARD4 and STARD6 immunoreactive proteins in different human ovarian sections for almost 15 different patients by immunohistochemistry. We localized STARD4 and STARD6 protein in almost 43 slides for human ovarian follicles at different stages. For corpus luteum, we studied around 23 slides of different human ovarian sections, while only 10 slides was examined for corpus albicans. The brown signal was considered positive.

Pregnenolone values from the COS-F2 assay were normalized for the protein content in the wells. Pregnenolone experiments were repeated three times with three different cell batches. All raw data was natural log (ln) transformed. Data for 3.1 vector, STARD4-WT, and STARD4-trunc were subjected to repeated measure ANOVA followed by Tukey's multiple comparison test. STARD1 a positive control was compare to 3.1 vector using Paired test. P value  $\leq 0.05$  was considered significant.

## Chapter III

### Results

#### **3.1 Detection of STARD4 and STARD6 mRNAs and protein in human ovarian tissues**

To evaluate the presence and relative abundance of STARD4 and STARD6 mRNA and protein levels in different human ovarian tissues, quantitative PCR and Western blots were performed. The ovarian biopsies contained ovarian cortex containing follicular tissue, a new corpus luteum (corpus hemorrhagicum (CH)), a mature corpus luteum (CL), or a degenerative corpus luteum (corpus albicans). Most of the corpus luteum tissue pieces had some adjacent stromal tissue attached, because we were unable to remove it from the frozen specimen without thawing. As normal human ovarian tissue is very hard to obtain, we do not have enough samples to analyze for statistics, and therefore present the data of the individual samples that we have available. STARD4 and STARD6 mRNA levels were extrapolated from a standard curve and normalized for their respective house-keeping gene TBP (Figure 3.1). STARD4 mRNA level is higher than STARD6 mRNA in both follicular and luteal tissues with the exception of the single degenerative corpus luteum. The level of STARD4 mRNA was highest in three of the four functional luteal structures which include CH and CL. The level of STARD6 mRNA was detected in all the ovarian tissues samples, but showed no expression trend with tissue type, although its level was highest in the degenerative corpus luteum sample.

Figure 3.2 represents the relative level of STARD4 and STARD6 proteins in human ovarian tissues as assessed by Western. These tissues were from most of the same ovarian samples used in Fig. 3.1. The Western blots show a STARD4 protein band in follicular phase cortex and luteal ovarian tissues with approximate size of 30 kDa. STARD6 with size around 43 kDa was also present in all ovarian tissues examined. Because the ovarian tissue samples were not purely follicles or corpus luteum tissue, we next examined tissue sections of human ovary using immunohistochemistry to localize STARD4 and STARD6 in different ovarian cell types and structures.

Figure 3.3 to 3.7 represent immunohistochemical microscopic images of human ovarian tissue sections containing various follicular and luteal structures including primordial follicles, unilaminar preantral follicles, multilaminar preantral follicles, antral follicles of different sizes, corpora hemorrhagica, corpora lutea, and corpora albicantia. Preliminary studies were performed with ovarian tissue sections and different dilutions of antibodies to determine the appropriate dilution of antibody to use in subsequent experiments. The signal of STARD4 and STARD6 was visualized as a brown color. Incubation of tissue sections with secondary antibody only gave no signal (Figures 3.3; 3.5; 3.6; 3.7: A, B, C; Figure 3.4. A).

The rabbit anti-STARD4 polyclonal antibody gave a strong signal with a concentration of 1:100. The granulosa and theca follicular cells of antral follicles were stained positively as were their oocytes (Figure 3.3 E, F and Figure 3.4 B), indicating the presence of immunoreactive STARD4 protein. Conversely, the flat epithelial cells surrounded the primordial follicles were not stained even though their oocyte still stained (Figure 3.3 D). The corpus luteum (Figure 3.5; 3.6 D, E, F) had a strong immunopositive

signal, with the cytoplasm of the luteal cell being stained lighter than the nucleus. Cells with the appearance of macrophages, the endothelium of blood vessels, and some red blood cells in the Figure 3.7. F were stained in the most sections. The corpus albicans, which is the degenerative form of corpus luteum, was not stained; additionally, the atretic follicles or degenerative follicles were also not stained (Figure 3.7, D, E).

For STARD6, granulosa and theca cells of antral and advanced follicles were positively stained by rabbit anti-STARD6 polyclonal antibody at a concentration of 1:100 (Figure 3.3 H, I and Figure 3.4 C). The positive signal was observed in the corpus luteum as homogenous distribution in the cytoplasm with dark nuclear staining (Figure 3.5 and 3.6 G, H, I), while the corpus albicans and atretic follicles were not stained (Figure 3.7, G, H). The endothelium cells of blood vessels and some RBCs were positively stained too (Figure 3.7, I).

To determine the specificity of STARD4 and STARD6 antibodies, we performed the immunohistochemistry with STARD4 or STARD6 antibodies after preabsorbing them with their respective blocking peptides. The ovarian tissue sections, were incubated with preabsorbed STARD4 antibody, showed reduced signal intensity in granulosa, theca (Figure 3.3, J), and luteal cells, even though the signal was not completely abolished. For STARD6, even though the signal was not abolished completely, there was reduced signal intensity between the slides treated with preabsorbed STARD6 antibody and the ones treated with non-preabsorbed STARD6 antibody (Figure 3.3, K).

### **3.2 Subcellular localization of STARD4 in transfected COS-1 cells by immunofluorescence microscopy**

The results in this section are with GRP78 and STARD4 are preliminary and have not been completely replicated (the experiment was repeated only two times). COS-1 cells were transfected with a commercially obtained expression plasmid containing the predicted wildtype human STARD4 cDNA linked to a myc-DDK tag to yield a fusion protein. The transfected COS-1 cells were utilized to probe for GRP78, an endogenous marker for the endoplasmic reticulum, and STARD4 using antibodies and confocal fluorescent microscopy. The immunoreactivity for STARD4 protein in COS-1 cells was localized throughout the cytoplasm and nucleus with the STARD4 primary antibody, whereas GRP78 antibodies showed a bright green signal in the cytoplasm adjacent to the nucleus (Figure 3.8). There was no evidence of co-localization of the two labels which would have been observed by a yellow signal upon merging the two images. Because of this negative result and the difficulty we experienced in optimizing antibodies for use in the primary ovarian cells, this part of the project was stopped.

### **3.3 Human luteinized granulosa cells express multiple STARD4 mRNA transcripts**

We cloned STARD4 transcripts from human luteinized granulosa cells in order to be able to express their proteins and determine their molecular mass. A cDNA library was constructed from poly (A) RNA, which was purified from pooled total RNA isolated from pooled cultured hGCs. After multiple trials of RACE-PCR, we amplified various products by 5' and 3' RACE-nested-PCR for hSTARD4. We used 5' RACE-nested-PCR product sequences and NCBI reference sequence entry XM\_005271881.1 to design the upstream primer to amplify the full-length product. One product of 3' RACE-nested-PCR

was used with NCBI reference sequence entry XM\_005271884.1 to design the downstream primer to isolate full-length STARD4 transcripts. The sequences of 5' and 3' RACE products are not shown.

We found a variation in the exon 1 sequence of two transcripts, but this was in non-coding exon 1, which would not affect the translated protein. Figure 3.9 (A) represents a diagram of the two major mRNA transcripts from human STARD4 isolated from hGCs, and Figure 3.9 (B) represents their cDNA sizes as visualized by agarose gel. The first STARD4 transcript possesses all six exons of human STARD4 mRNA according to NCBI reference sequence entry NM\_139164.1. The first transcript of STARD4 has length of 715 base pairs and predicted to yield full-length STARD4 protein; therefore we called the first transcript the full-length or wild-type transcript (STARD4-WT). The second transcript possesses an exon 4 deletion, which introduces a premature stop codon and is predicted to yield one or more truncated proteins. The exon 4 deletion transcript has length of 588 base pairs and Figure 3.10 shows the alignment and the matching of STARD4-WT and exon 4 deletion transcripts to the human STARD4 mRNA obtained from Genbank.

### **3.4 Determining the size of recombinant proteins produced from human full-length STARD4 and exon four-deleted STARD4 mRNA isolated from hGC**

Transfected COS-1 cells were utilized to evaluate the expression of STARD4 recombinant proteins and their sizes generated from the cloned cDNA derived from human luteinized granulosa cells mRNA transcripts. Figure 3.11 shows the predicted size of recombinant STARD4 proteins and their sequences. The full-length protein, which was produced from the full-length STARD4 transcript, and the putative truncated

proteins produced from the exon 4 deleted STARD4 transcript. The expected size for a full-length protein is 205 amino acids, which matches the wild type STARD4 protein reported in Genbank, with a predicted molecular weight of 23.52 kDa. The truncated STARD4 protein was predicted to produce two possible different sized proteins based on analysis of reading frames, with one having 55 amino acids with a predicted molecular weight of 6.37 kDa, because the exon 4 deletion transcript introduced premature stop codon. The reading frame two produces a protein with 107 amino acids having a predicted size of 12.16 kDa. Our STARD4 antibody recognizes the N-terminus so would likely not detect the longer truncated protein if translated.

To confirm protein expression, whole cell extracts were isolated from the transfected COS-1 cells. The transfected P450scc complex fusion protein was detected in the cells which meant all the plasmids were successfully transfected and expressed. The analysis of protein, immunoblot on Figure 3.12 showed only the wild-type STARD4, where the band size approximately 24 kDa for the COS-1 cells transfected with full-length STARD4 plasmid. Conversely, the two predicted sizes of truncated protein did not show on the gel even after long exposure. This negative result may mean that the protein was made and quickly degraded, the intensity of exposure was not enough, or the protein was not made. It is likely that the antibody, which targets the N-terminus, would not detect the trunc-1 product. For that, we need to perform more experiments to detect the truncated STARD4 protein.

### **3.5 Human full-length STARD4 recombinant protein is able to facilitate *de novo* steroidogenesis in the COS-1 F2 assay**

The COS-1 F2 assay was used to evaluate the steroidogenic ability of the recombinant STARD4 full-length and exon 4 deleted transcript proteins. STARD4 expression vectors transfected with the F2 plasmid and the pregnenolone (P5) levels were measured in the media by ELISA. STARD1 has been shown to increase pregnenolone production in F2-transfected COS-1 cells, which served as a positive control. The experiment was replicated three times. Pregnenolone levels were normalized to the concentration of proteins in the well (ng P5/ng protein).

Figure 3.13 represents the pregnenolone levels for transfected COS-1 cells cultures. COS-1 cells transfected with P450<sub>scc</sub> and the empty expression vector only (pcDNA3.1) showed very low concentration of pregnenolone. The pregnenolone production was significantly increased ( $P < 0.001$ ) in the STARD1 transfected cells with a mean increase of 9.8-fold compared to the empty vector control. In the full-length STARD4 transfected cells, the increase in pregnenolone was statistically significant ( $P < 0.05$ ) at a mean 3.8-fold compared to the empty control vector indicating that the full-length STARD4 protein is able to facilitate cholesterol entry into the mitochondria to promote steroidogenesis. Even though the pregnenolone level produced by STARD4-truncated protein was increased by 2.1-fold, it was not statistically significant ( $P > 0.05$ ) compared to the empty vector only.

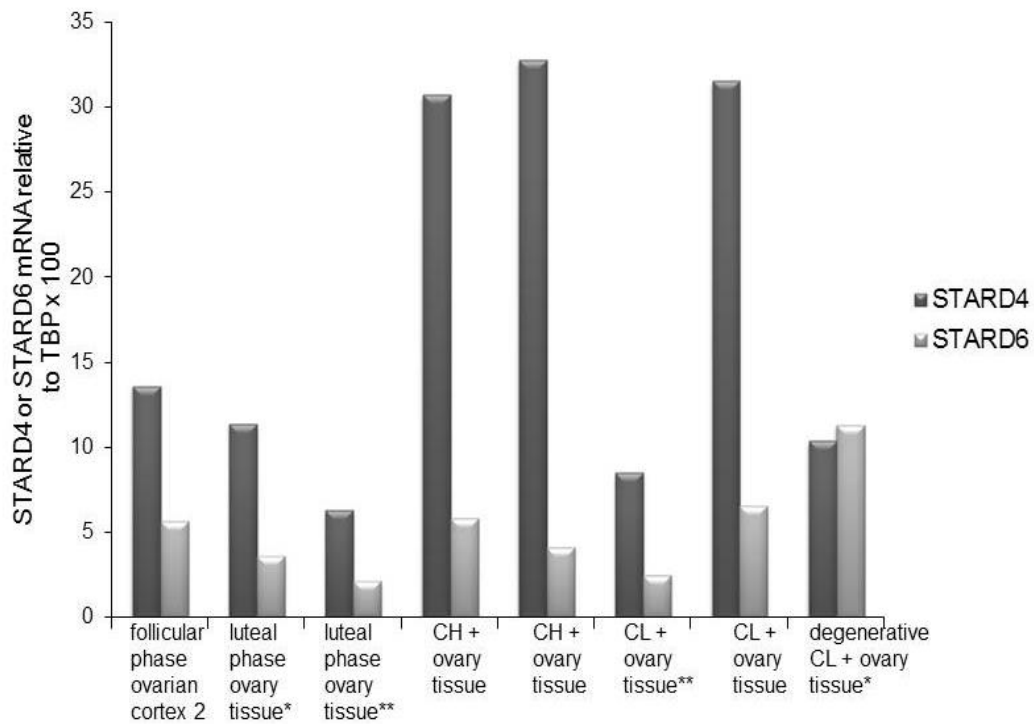


**Figure 3.1. STARD4 and STARD6 mRNA expression in human ovarian tissues.** The RNA was isolated from ovarian tissues at various stages (follicular and luteal phases), and mRNA levels was measured by real-time PCR. CL (Corpus luteum); CH (Corpus hemorrhagicum). (\* / \*\*) indicate that the tissue samples with same asterisks were taken from the same ovary. STARD4 and STARD6 mRNA levels was normalized to TATA box-binding protein (TBP, an unregulated house-keeping gene).

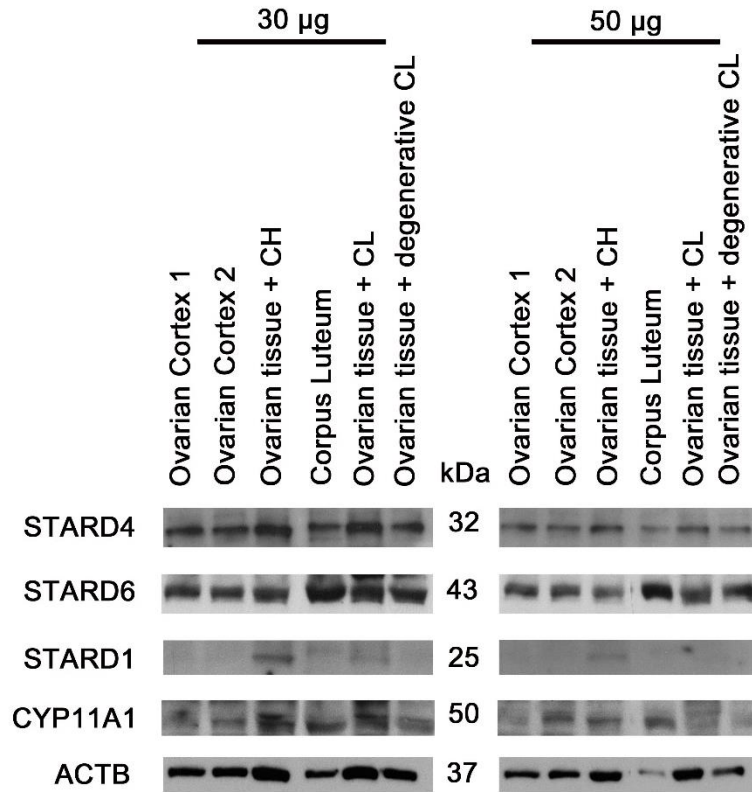


**Figure 3.2. Western blot analyses of STARD4 and STARD6 proteins in human ovarian tissue samples.** The blots show the expression of STARD4 and STARD6 proteins in all ovarian tissue sections. The proteins samples represent whole cell extracts from ovarian tissue sections indicated. The whole proteins were separated by SDS-polyacrylamide gel electrophoresis using 4-20% gradient gels and transferred to PVDF membrane and probed with antibodies for the indicated proteins. The right membrane has 50 µg of proteins, while the amount of the same proteins in the left membrane is 30 µg. The tissue sections contained mix of stromal and follicular tissues; or stromal and luteal tissues. Ovarian cortex tissue (contained small and medium antral follicles); CL (Corpus luteum); CH (Corpus hemorrhagicum).

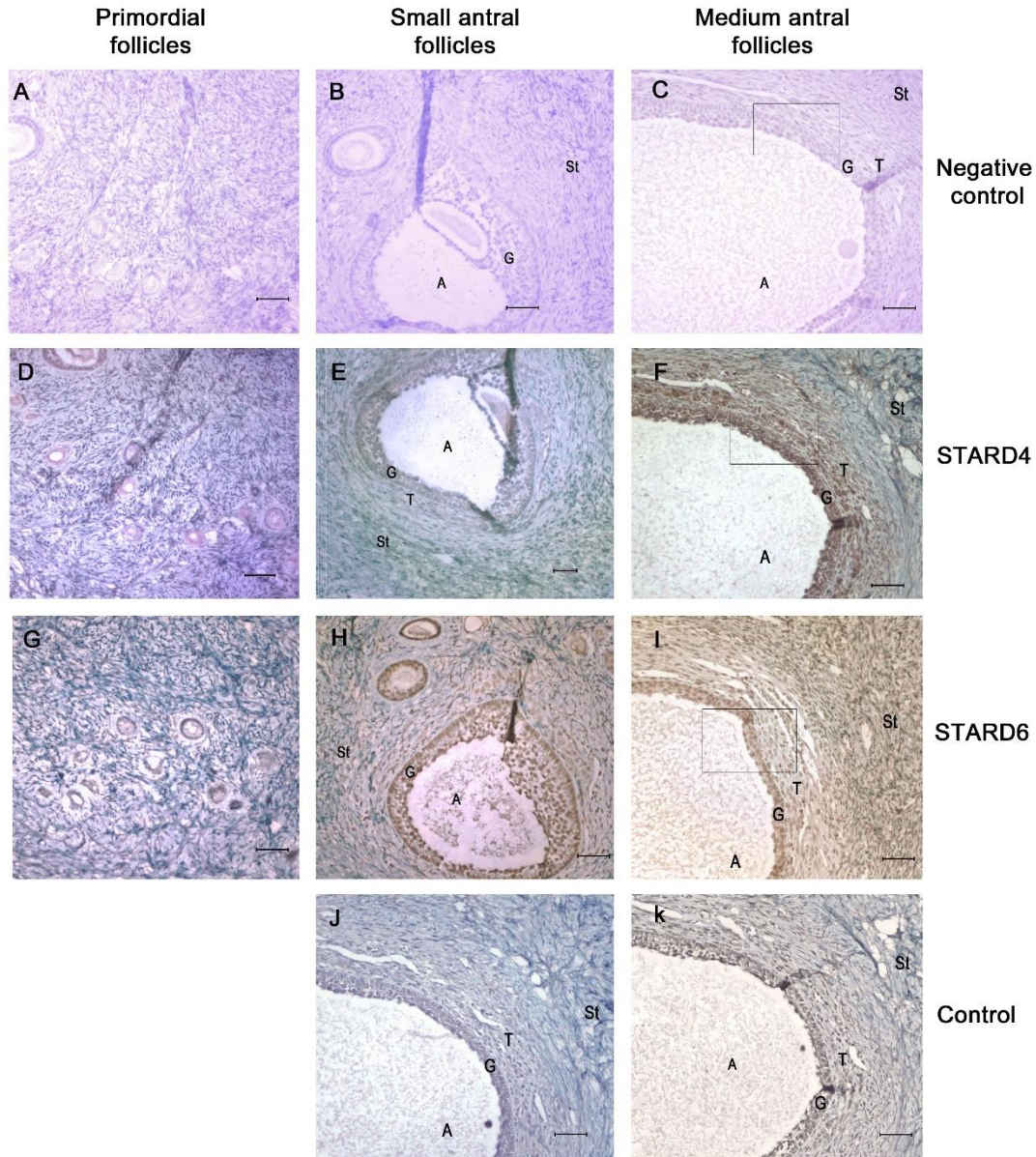


**Figure 3.3. Immunolocalization of STARD4 and STARD6 in human ovarian tissue sections.** A, D, G represent biopsies of ovarian cortex showing primordial and small preantral follicles and stromal tissue. B, E, H represent small antral follicles. C, F, I, K, J represent medium antral follicles. A-C negative control sections probed with secondary antibody only. D-F sections probed with STARD4 primary antibody. G-I probed with STARD6 primary antibody. J and K are a control; where (J) was probed with STARD4 blocking peptide, and (K) probed with STARD6 blocking peptide. The positive staining is shown in brown. All sections were counterstained with hematoxylin. The magnification for all sections is 20X with scale bar of 65  $\mu$ m. **A**= Antrum, **G**= granulosa cells, **T**= theca cells, **St**= stromal tissue. The small square regions in the right side column are enlarged on the next figure.

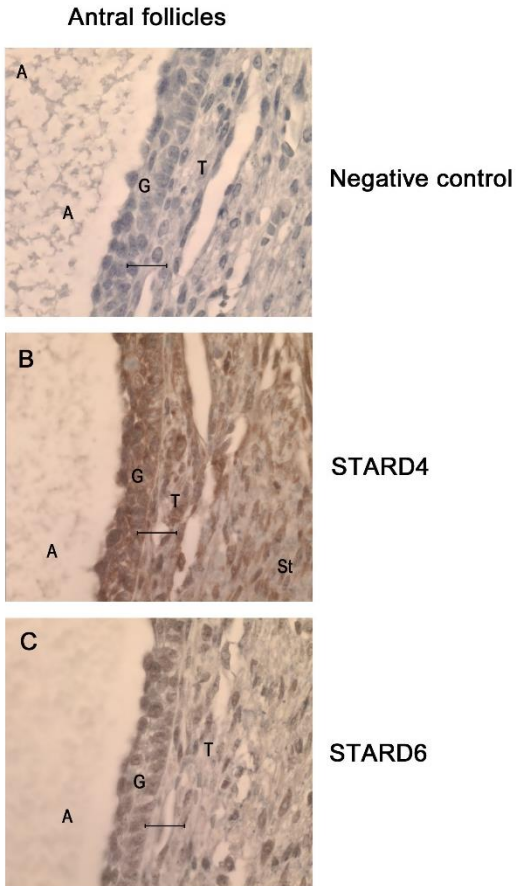


**Figure 3.4. Immunolocalization of STARD4 and STARD6 proteins in human antral follicles.** The pictures represent 63X magnification of the small square on the previous figure. Image A represents a negative control which is probed with secondary antibody only. The section B is probed with STARD4 antibody. The section C is probed with STARD6 antibody. **A**= antrum, **G**= granulosa cells, **T**= theca cells, **St**= stromal tissue. The positive staining is shown in brown. All sections were counterstained with hematoxylin. The scale bar is 20  $\mu$ m. The light settings were the same for all images in this figure.

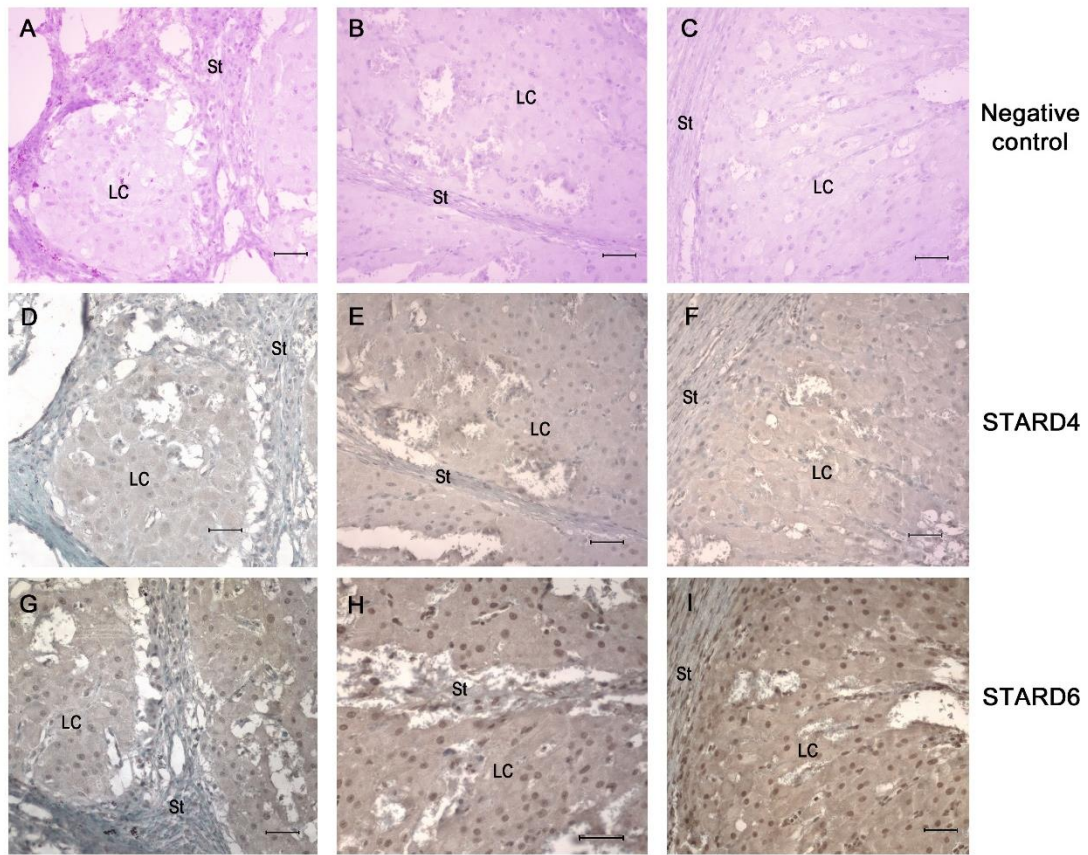


**Figure 3.5. Immunolocalization of STARD4 and STARD6 in the corpus luteum of human ovarian tissues.** A-C negative control sections probed with secondary antibody only. D-F sections probed with STARD4 primary antibody. G-I sections are probed with STARD6 primary antibody. The positive staining is shown in brown. All sections were counterstained with hematoxylin. The magnification is 20X with scale bar of 65  $\mu$ m. LC= luteal cells, St= stromal tissue.

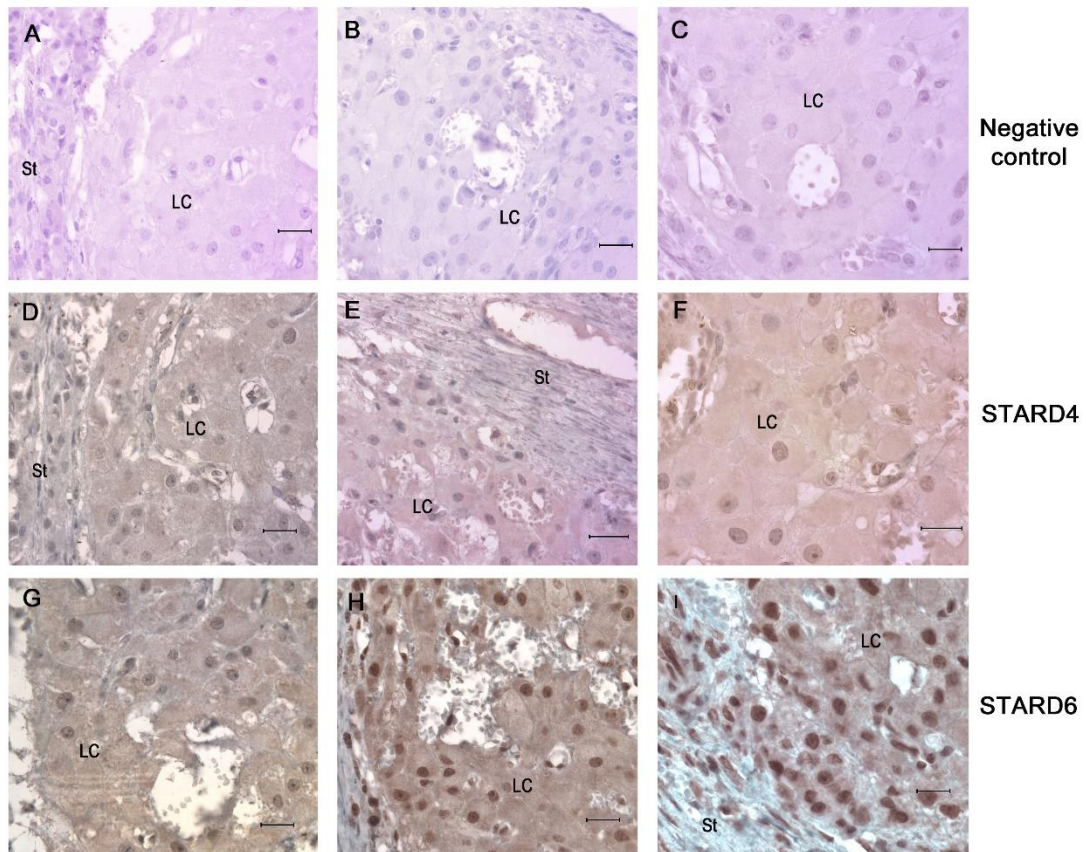


**Figure 3.6. Immunolocalization of STARD4 and STARD6 in the corpus luteum of human ovarian tissues.** A-C negative control sections probed with secondary antibody only. D-F sections probed with STARD4 primary antibody. G-I sections are probed with STARD6 primary antibody. The positive staining is shown in brown. All sections were counterstained with hematoxylin. The magnification for (A, B, D, E, G, H) is 40X with scale bar of 25  $\mu\text{m}$ ; while for (C, F, I) is 63X with scale bar of 16  $\mu\text{m}$ , LC= luteal cells, St= stromal tissue.

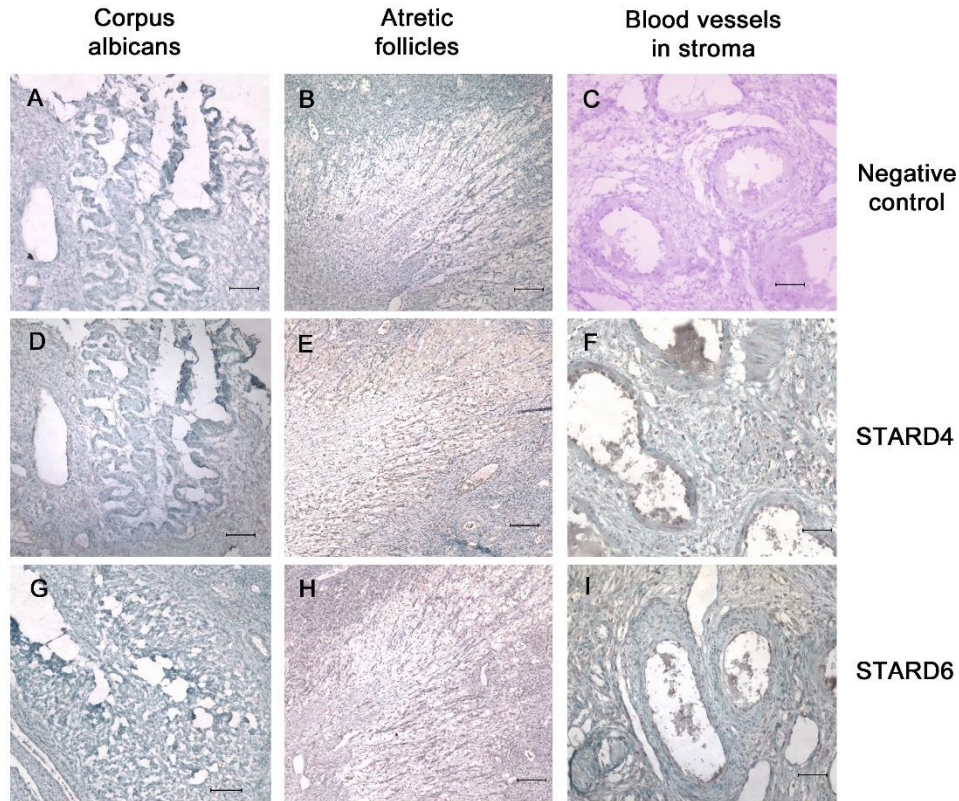


**Figure 3.7. Immunolocalization of STARD4 and STARD6 in human ovarian tissue sections.** A, D, G represent biopsies obtained from ovarian cortex of corpus albicans. B, E, H represent atretic follicles. C, F, I represent blood vessels in ovarian stroma with 20X magnification and scale bar of 65  $\mu\text{m}$ . The magnification of A, B, D, E, G, H sections is 10X with scale bar of 100  $\mu\text{m}$ . A-C negative control sections probed with secondary antibody only. D-F sections probed with STARD4 primary antibody. G-I sections probed with STARD6 primary antibody. The positive staining is shown in brown. All sections were counterstained with hematoxylin.

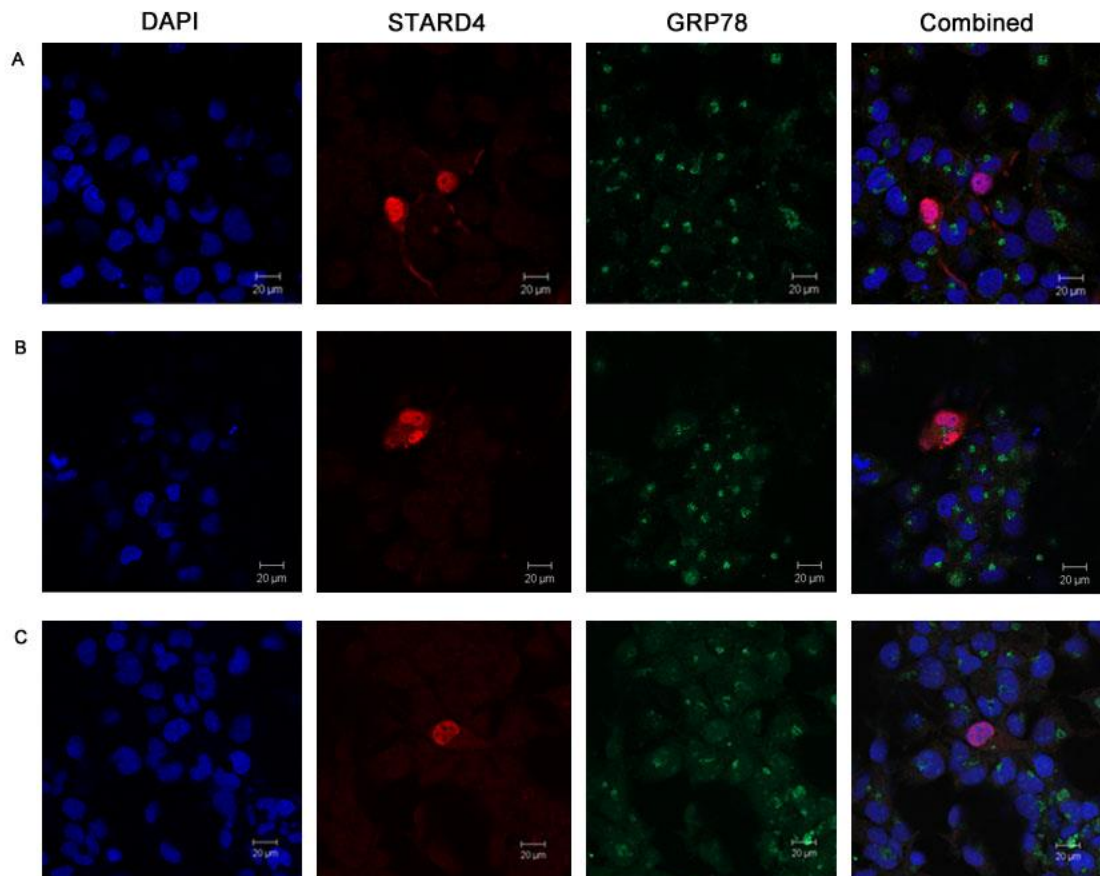
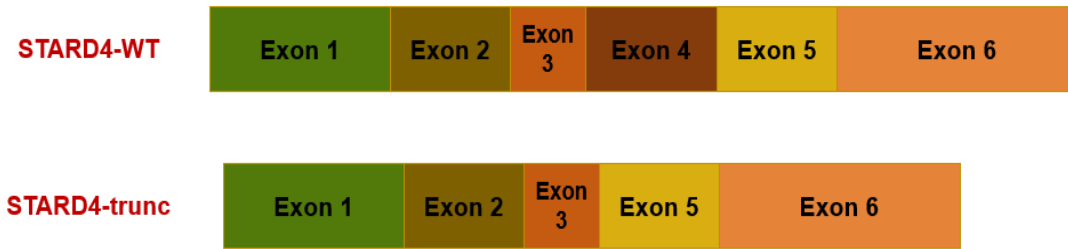


**Figure 3.8. Immunofluorescence confocal microscopy assessment of recombinant STARD4 and endogenous GRP78 proteins in transfected COS-1 cells.** COS-1 cells were transfected with myc-DKK-tagged STARD4 expression plasmid then prepared for double labeling immunofluorescence confocal microscopy. A-C each represents 40X magnification of the same visual field under the microscope. DAPI is shown as blue color staining the nucleus. STARD4 primary antibody was detected as the red color of CY3 donkey anti-rabbit secondary antibody. GRP78 primary antibody detected by CY2 donkey anti-goat secondary antibody is shown in green. Scale bar is 20 μm.

(A)



(B)

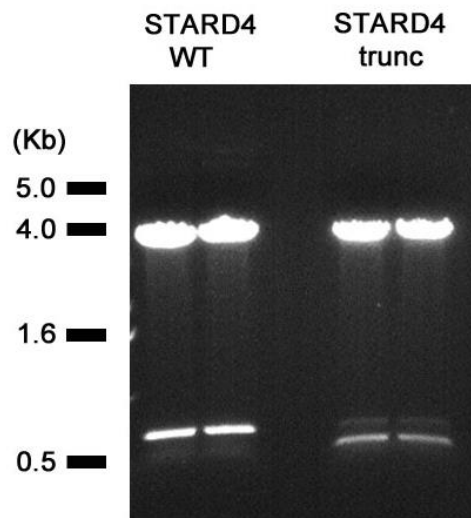


**Figure 3.9. Schematic view of the major mRNA transcripts of human STARD4 which were isolated from human granulosa cells and their sizes on agarose gel.** (A) The predicted exons of the STARD4 transcripts are shown according to GenBank NCBI Reference Sequence entry NM\_139164.1. The STARD4 wild-type (WT) possess all six exons of human STARD4 mRNA illustrated here with boxes and codes for a 205 amino acids protein. The STARD4-trunc transcript is lacking exon 4 and is predicted to produce a 55 or 107 amino acid protein.

(B) An agarose gel showing different STARD4 cDNA sizes. The cloned cDNAs were digested from the PCR2.1 cloning vector with EcoRI and separated using 1.2% agarose gel. The gel purified cDNA inserts were subsequently inserted into the pcDNA3.1 plasmid for expression purposes.

**STARD4 mRNA** CTTCCACGTCCTTGCTTCACCTCAGGTAAAGAGAGAAGTAATGGAAGGCCTGTCTGATGT  
**STARD4-trunc** CTTCCACGTCCTTGCTTCACCTCAGGTAAAGAGAGAAGTAATGGAAGGCCTGTCTGATGT  
**STARD4-WT** CTTCCACGTCCTTGCTTCACCTCAGGTAAAGAGAGAAGTAATGGAAGGCCTGTCTGATGT  
 \*\*\*\*\*

**STARD4 mRNA** TGCTTCTTTTGCAACTAAACTTAAAAACACTCTCATCCAGTACCATAGCATTGAAGAAGA  
**STARD4-trunc** TGCTTCTTTTGCAACTAAACTTAAAAACACTCTCATCCAGTACCATAGCATTGAAGAAGA  
**STARD4-WT** TGCTTCTTTTGCAACTAAACTTAAAAACACTCTCATCCAGTACCATAGCATTGAAGAAGA  
 \*\*\*\*\*

**STARD4 mRNA** TAAGTGCGAGTTGCTAAGAAAACGAAAGATGTAAGTGTGGAGAAAACCCTCAGAAGA  
**STARD4-trunc** TAAGTGCGAGTTGCTAAGAAAACGAAAGATGTAAGTGTGGAGAAAACCCTCAGAAGA  
**STARD4-WT** TAAGTGCGAGTTGCTAAGAAAACGAAAGATGTAAGTGTGGAGAAAACCCTCAGAAGA  
 \*\*\*\*\*

**STARD4 mRNA** ATTTAATGGATATCTCTACAAAGCCCAAGGTGTTATAGATGACCTTGTCTATAGTATAAT  
**STARD4-trunc** ATTTAATGGATATCTCTACAAAGCCCAAGGTGTTATAGATGACCTTGTCTATAGTATAAT  
**STARD4-WT** ATTTAATGGATATCTCTACAAAGCCCAAGGTGTTATAGATGACCTTGTCTATAGTATAAT  
 \*\*\*\*\*

**STARD4 mRNA** AGACCATATACGCCCAGGGCCTTGTGCTTTGGATTGGGACAGCTTGATGACTTCTTTGGA  
**STARD4-trunc** AGACCATATACGCCCAGGGCCTTGTGCTTTGGATTGGGACAGCTTGATGACTTCTTTGGA  
**STARD4-WT** AGACCATATACGCCCAGGGCCTTGTGCTTTGGATTGGGACAGCTTGATGACTTCTTTGGA  
 \*\*\*\*\*

**STARD4 mRNA** TATTCTGGAGAACTTGAAGAGAAATTGCTGTGTGATGCGTTACACTACTGCTGGTCAGCT  
**STARD4-trunc** TATTCTGGAGAACTTGAAGAGAAATTGCTGTGTGATGCGTTACACTACTGCTGGTCAGCT  
**STARD4-WT** TATTCTGGAGAACTTGAAGAGAAATTGCTGTGTGATGCGTTACACTACTGCTGGTCAGCT  
 \*\*\*\*\*

**STARD4 mRNA** TTGGAATATAAATTTCCCAAGAGAATTTGTTGATTTCTCCTATACTGTGGGCTATAAAGA  
**STARD4-trunc** TTGGAATATAAATTTCCCAAGAGAATTTGTTGATTTCTCCTATACTGTGGGCTATAAAGA  
**STARD4-WT** TTGGAATATAAATTTCCCAAGAGAATTTGTTGATTTCTCCTATACTGTGGGCTATAAAGA  
 \*\*\*\*\*

**STARD4 mRNA** AGGGCTTTTATCTTGTGGAATAAGTCTTGACTGGGATGAAAAGAGACCAGAATTTGTTTCG  
**STARD4-trunc** AGGGCTTTTATCTTGTGGAATAAGTCTTGACTGGGATGAAAAGAGACCAGAATTTGTTTCG  
**STARD4-WT** AGGGCTTTTATCTTGTGGAATAAGTCTTGACTGGGATGAAAAGAGACCAGAATTTGTTTCG  
 \*\*\*\*\*

**STARD4 mRNA** AGGATATAACCATCCCTGTGGTTGGTTTTGTGTTCCACTTAAAGACAACCCAAACCAGAG  
**STARD4-trunc** AGGATATAACCATCCCTGTGGTTGGTTTTGTGTTCCACTTAAAGACAACCCAAACCAGAG  
**STARD4-WT** AGGATATAACCATCCCTGTGGTTGGTTTTGTGTTCCACTTAAAGACAACCCAAACCAGAG  
 \*\*\*\*\*

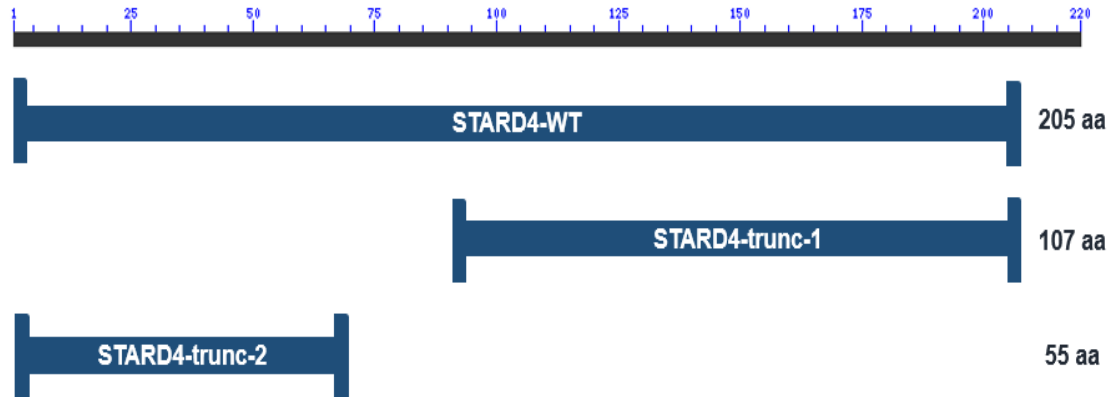
**STARD4 mRNA** TCTTTTGACAGGATATATTCAGACAGATCTGCGTGGGATGATTCCTCAGTCTGCGGTAGA  
**STARD4-trunc** TCTTTTGACAGGATATATTCAGACAGATCTGCGTGGGATGATTCCTCAGTCTGCGGTAGA  
**STARD4-WT** TCTTTTGACAGGATATATTCAGACAGATCTGCGTGGGATGATTCCTCAGTCTGCGGTAGA  
 \*\*\*\*\*

**STARD4 mRNA** TACAGCCATGGCAAGCACTTTAACCAACTTCTATGGTGATTTACGAAAAGCTTTATGAGA  
**STARD4-trunc** TACAGCCATGGCAAGCACTTTAACCAACTTCTATGGTGATTTACGAAAAGCTTTATGAGA  
**STARD4-WT** TACAGCCATGGCAAGCACTTTAACCAACTTCTATGGTGATTTACGAAAAGCTTTATGAGA  
 \*\*\*\*\*

**STARD4 mRNA** GGCAAATAACATTCAAACTTGTAGTACTACAGATCAACTCTCTCAGCTACATGGCCTGTA  
**STARD4-trunc** GGCAAATAACATTCAAACTTGTAGTACTACAGATCAACTCTCTCAGCTACATGGC-----  
**STARD4-WT** GGCAAATAACATTCAAACTTGTAGTACTACAGATCAACTCTCTCAGCTACATGGC-----  
 \*\*\*\*\*

**Figure 3.10. The homology and the alignment of STARD4-WT and STARD4 cDNAs.** The homology of STARD4-WT and STARD4 cDNA from GenBank NCBI Reference Sequence entry [ref|NM\\_139164.1|](#). The STARD4-WT transcript is 715 base pair in length. **ATG** = starting codon, **TGA** = stop codon. Alignment of STARD4 wild-type (WT) and truncated (STARD4-trunc) transcripts to STARD4 mRNA using Multiple Sequence Alignment by CLUSTALW. (\*\*\*) indicate complete matching (100%), while (-----) indicates the exon 4 deletion in STARD4-truncated transcript.

(A)



(B)

HS-STARD4	MEGLSDVASFATKLNKNTLIQYHSIEEDKWRVAKKTKDVTVWRKPSEEFNGYLYKAQGVID
STARD4-WT	MEGLSDVASFATKLNKNTLIQYHSIEEDKWRVAKKTKDVTVWRKPSEEFNGYLYKAQGVID
STARD4-trunc1	-----
STARD4-trunc2	MEGLSDVASFATKLNKNTLIQYHSIEEDKWRVAKKTKDVTVWRKPSEEFNGYLIIV-----
HS-STARD4	DLVYSIIDHIRPGPCRLDWDLSLMTSLDILENFEENCCVMRYTTAGQLWNIISPREFVDFS
STARD4-WT	DLVYSIIDHIRPGPCRLDWDLSLMTSLDILENFEENCCVMRYTTAGQLWNIISPREFVDFS
STARD4-trunc1	-----MRYTTAGQLWNIISPREFVDFS
STARD4-trunc2	-----
HS-STARD4	YTVGYKEGLLSCGISLDWDEKRPEFVRGYNHPCGWFCVPLKDNPNQSLLTGYIQTDLRGM
STARD4-WT	YTVGYKEGLLSCGISLDWDEKRPEFVRGYNHPCGWFCVPLKDNPNQSLLTGYIQTDLRGM
STARD4-trunc1	YTVGYKEGLLSCGISLDWDEKRPEFVRGYNHPCGWFCVPLKDNPNQSLLTGYIQTDLRGM
STARD4-trunc2	-----
HS-STARD4	IPQSAVDTAMASTLTNFGDLRKAL
STARD4-WT	IPQSAVDTAMASTLTNFGDLRKAL
STARD4-trunc1	IPQSAVDTAMASTLTNFGDLRKAL
STARD4-trunc2	-----

**Figure 3.11. Diagram illustrating the predicted sizes of STARD4 wild-type and truncated proteins and their alignment with Homo sapiens STARD4 protein. (A)** Using the Sequence Manipulation Suite and BLAST to predict the sizes of the proteins. STARD4-WT yields a protein of 205 amino acids (aa) with molecular weight of 23.52 kDa. STARD4-truncated transcript is predicted to produce two short proteins, because of a premature stop codon and according to different reading frames. STARD4-trunc-1 matches 107 aa of human STARD4 protein with predicted molecular weight of 12.16 kDa. STARD4-trunc-2 consists of 55 aa with molecular weight of 6.37 kDa.

**(B)** The alignment of STARD4-WT, and both isolated STARD4-truncated protein sequences with Homo sapiens STARD4 protein using Multiple Sequence Alignment by CLUSTALW. (HS-STARD4) is a Homo sapiens STARD4 protein sequence. The sequence of STARD4-WT completely matches the Homo sapiens STARD4. STARD4-trunc-1 matches the last 107 amino acids, while the STARD4-trunc-2 matches the first 55 amino acids of Homo sapiens STARD4 isoform CRA\_e with reference ID [gb|EAW49030.1|](#).

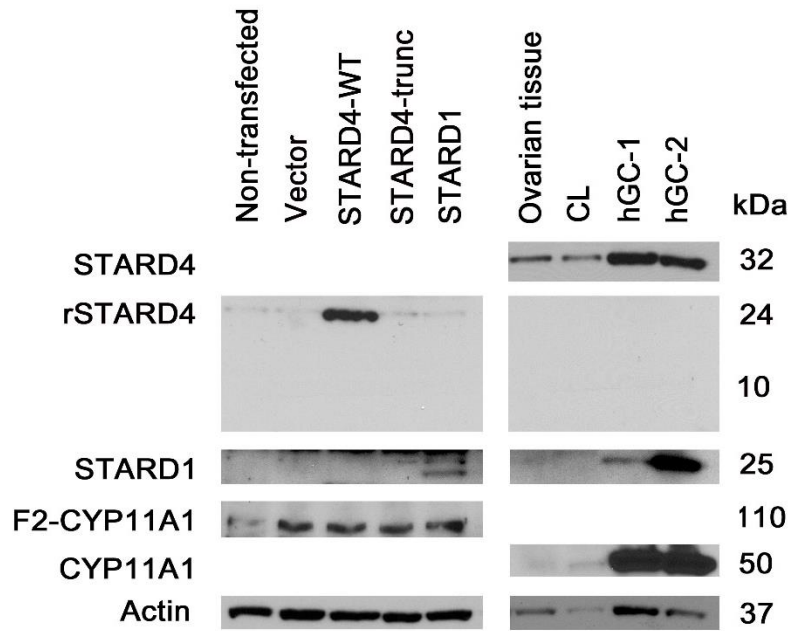


**Figure 3.12. Western blot for comparing human recombinant STARD4 and endogenous STARD4 proteins.** The left panel is transfected COS-1 cells, and the right panel is human ovarian tissues and human luteinized granulosa cells (hGC). Both panels are from the same blot. All samples were loaded with 25  $\mu$ g protein, and probed with STARD4, STARD1, and CYP11A1 rabbit primary antibodies. Actin reflects protein loading. (CL) Corpus luteum.

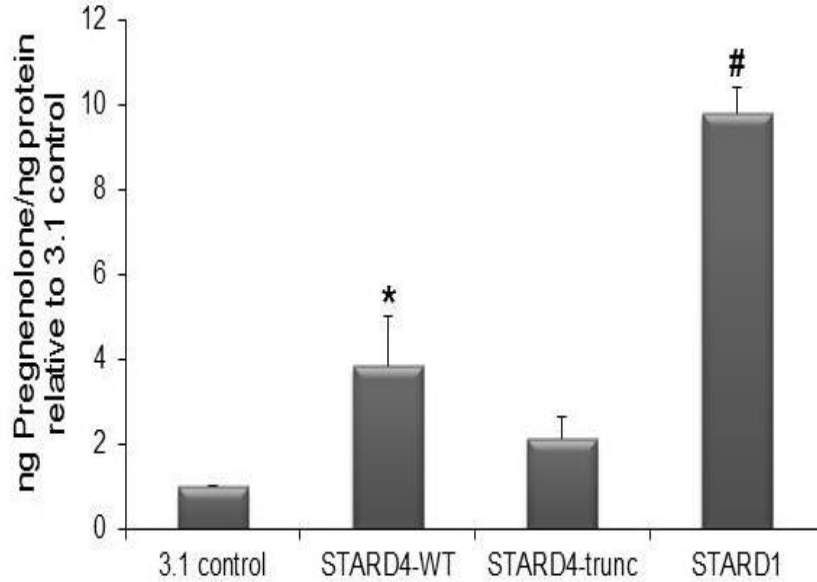


**Figure 3.13. COS-F2 steroidogenic assay to assess the pregnenolone production by recombinant STARD4 proteins derived from human granulosa cells transcripts.** COS-1 cells were transfected with equimolar amounts of plasmids encoding recombinant STARD4 (wildtype or trunc), STARD1 proteins, or vector only along with the F2 plasmid which encodes the p450 cholesterol side chain cleavage enzyme complex as a fusion protein. Pregnenolone was measured in the media by P5 ELISA from three separate transfection experiments. Comparison of STARD4 conditions with 3.1 control (empty expression vector) were performed. Asterisk indicates mean is significantly different from 3.1 control by ANOVA and Tukey's Multiple Comparison test,  $P < 0.05$ . # indicates treatment is significantly different from 3.1 control by paired t-test,  $P < 0.001$ .

## **Chapter IV**

### **Discussion**

In this study, STARD4 and STARD6 proteins were localized in human ovarian steroidogenic cells (granulosa cells, thecal cells, and luteal cells). Only two published studies have investigated STARD4 and STARD6 expression in the ovary. Our results are consistent with that of Skiadas et al (2012) that found STARD4 mRNA in human granulosa cells isolated from women undergoing assisted reproduction. In addition, a previous study by our lab detected STARD6 in porcine ovarian granulosa cells, which is similar to our finding in the human ovary (LaVoie et al. 2014). In the pig studies, STARD6 mRNA had much higher expression in all ovarian tissues than in the human, as determined from standard curves. In pig, STARD6 mRNA and protein levels in mid-luteal phase or functional corpus luteum were significantly higher than follicles and granulosa cells; this was not the case in human ovarian tissues where STARD6 mRNA was similar between ovarian tissue with follicles and different stages of functional corpus luteum. Our current data with STARD4 mRNA in human ovarian tissues more closely approximates what has been reported for pig STARD6 mRNA. Despite our higher levels of STARD4 mRNA in the majority of human functional corpora lutea assessed, there was no trend in STARD4 protein levels.

Like STARD1, which is a known major regulator of steroidogenesis, STARD4 and STARD6 can bind and transport cholesterol. Until recently, STARD4 and STARD6

were largely ignored as potential participants in steroidogenesis because they were not detected in the ovary, such as with STARD6, or the tissue distribution had not been characterized, such as with STARD4 (LaVoie et al. 2014; Soccio et al. 2005). The presence of these proteins in ovarian steroidogenic cells gives some suggestion that they could have a role in steroidogenesis. Other studies have found STARD4 in the cytoplasm of human THP-1 macrophages and Kupffer cells with a co-localization to ER areas enriched in acyl-coA cholesterol transferase-1.

STARD4 is highly regulated by sterol levels indicating that STARD4 has a role in maintaining intracellular cholesterol homeostasis (Rodriguez-Agudo et al. 2011). Structural studies for STARD6 have shown that STARD6 has folding and hydrophobic sterol-binding pocket similar to STARD1; interestingly, STARD6 also interacts with mitochondrial membranes (Bose et al. 2008). All together these findings suggest that STARD4 and STARD6 may have a role in providing cholesterol substrate to the mitochondria.

In order to determine the size of STARD4 protein from the mRNA of hLGC, we attempted to clone all the major transcripts of STARD4 using a combination of 5' and 3' RACE and traditional high fidelity PCR. We succeeded in isolating two major transcripts for STARD4 from pooled cultured human luteinized granulosa cell poly (A) mRNA. The longer full-length transcript possesses all six exons of STARD4 with length of 715 base pairs and is predicted to produce a full-length STARD4 protein of 205 amino acids with normal function. The full-length STARD4 transcript matches a previous cloned human transcript at the National Center for Biotechnology Information (<http://www.ncbi.nlm.nih.gov/>) under the reference sequence entry NM\_139164.1. While

the second shorter transcript possesses an exon 4 deletion that is predicted to yield 55 and/or 107 amino acid proteins. The second transcript has been found in fetal brain, bone marrow, and pulmonary endothelial artery (NCBI).

After we transfected the COS-1 cells with our two STARD4 transcripts, we were able to generate the full-length recombinant STARD4 protein from the longer cDNA. In our studies, the endogenous ovarian STARD4 yields a single band of an approximately molecular mass of 30 kDa. Based on amino acid sequence only, the predicted mass for the wild-type STARD4 protein should be 23.5 kDa. The full-length recombinant STARD4 protein has size of 24 kDa in COS cell lysates. Similar to our findings, human recombinant STARD4 protein expressed in BL21 E. coli cells had a size range between 22-27 kDa (Rodriguez-Agudo et al. 2008). The major protein band was found at 27 kDa with the Histidine tag. However, when the His tag was cleaved by enterokinase, the recombinant STARD4 protein run at around 22 kDa (Rodriguez-Agudo et al. 2008). Our data in human ovarian tissue and cultured granulosa cells identify a single protein band with an apparent molecular mass of approximately 30 kDa. This finding is similar to that of human placenta, where STARD4 protein also migrates at an apparent mass of 30 kDa (<http://www.avivasysbio.com/stard4-antibody-n-terminal-region-0aab09082.html>).

It is possible that posttranslational modifications (PTMs) alter the mass of the STARD4 protein made in granulosa cells. It may be that the endogenous STARD4 has phosphate groups as posttranslational modifications, which would increase the size of the protein by 80 Da for each added phosphate group (Seo and Lee 2003). Other PTMs which may occur and change the protein mass significantly are ubiquitination, which adds 8.5 kDa for each ubiquitin and acetylation which adds 42 Da for each acetyl group

added to a protein (Seo and Lee 2003). The PTM may occur ovarian cells but not in transfected COS cell thereby explaining why the recombinant STARD4 protein is smaller in size than the endogenous protein. To analyze the PTMs that change the size of our protein, we will have to use different techniques; for example, 2-D gel electrophoresis and/or mass spectrometry.

Whereas the full-length protein was detected in transfected COS cell lysates by Western blot, the truncated protein was not detected. Possible explanations for the lack of detection of the truncated protein are that the size of the predicted protein is very small and may not have resolved well on the Tris-HCl gels, the mRNA for or the truncated protein is degraded rapidly, or the protein may not be translated. To resolve these questions, we may need to run the protein lysates on Tris-Tricine gels for better resolution of small proteins, add proteasome inhibitor to the culture to inhibit protein degradation, or do PCR to insure that the mRNA of truncated STARD4 protein is transcribed. Another student in our laboratory has *in vitro* transcribed and translated the STARD4 plasmid constructs using a Wheat germ system and resolved the proteins on 16% Tris-Tricine-SDS-PAGE gels (Yahya and LaVoie, unpublished data). For the full-length STARD4 construct a protein of 22 kDa was observed. For the STARD4 construct lacking exon 4 protein two bands of approximately 3 kDa and 6 kDa were observed by Western blot using an N-terminal recognizing antibody. Further investigation is required know if these two bands are functionally active. Also should a C-terminal recognizing antibody become available in the future we can reprobe our blots.

We hypothesized that the full-length STARD4 transcript would produce a protein in COS-1 cells containing transfected components of the P450<sub>scc</sub> complex and that

STARD4 protein would increase pregnenolone production, and that the truncated protein would not be able to increase pregnenolone production. The full-length recombinant STARD4 protein shows steroidogenic ability in transfected COS-1 cells, which the pregnenolone production is increased by 3.8 fold. Our findings agree with a similar study in which transfected COS cells containing wild-type STARD4 and the genes for encoding the machinery to convert cholesterol to progesterone, increased progesterone production (Soccio et al. 2005). STARD4 protein also had a similar ability to transport cholesterol as STARD1 but not to the same amplitude (Soccio et al. 2005). These previous studies and our results indicate that STARD4 can somehow transport cholesterol into the mitochondria for *de novo* steroidogenesis. The truncated recombinant STARD4 protein did show a small degree of pregnenolone production, which is increased by 2.1-fold when compared to the empty vector. This increase was not statistically significant. In wild-type or full-length human STARD4 mRNA, exon one is noncoding, while the rest of the exons code the entire START domain (Soccio et al. 2002). Deletion of exon 4 in truncated STARD4 transcript would result in a truncated protein lacking the bulk of the START domain and likely be minimally active or functionally inactive, lacking the ability to transfer cholesterol.

There was no evidence of subcellular co-localization of STARD4 protein in transfected COS cells and ER marker, the GRP78 protein, using immunofluorescence microscopy; which infers that STARD4 protein is not localized to ER region where the GRP78 protein is located. We may need to try another ER marker such as calnexin, which is an integral protein of the endoplasmic reticulum and has a function as a chaperone. In a previous study, calnexin was co-localized with STARD4 in the cytoplasm

and ER of 3T3-L1 cells (Rodriguez-Agudo et al. 2011). We could also test co-localization with mitochondrial marker like VDAC2 or other vesicular markers.

Despite the ability of STARD4 and STARD6 to transfer cholesterol, StAR protein is still the most important protein to transfer the cholesterol from OMM into IMM for *de novo* steroidogenesis in adrenal gland and gonads. This is supported by the fact that loss of StAR is associated with CAH, a lethal condition if supplemental steroids are not given. However, some untreated patients with CAH initially have low levels of adrenal steroids which disappear with time (Miller 1997). This initial steroidogenesis could be due in part to partial activity of mutant StAR proteins in CAH. However, this finding of initial low steroid secretion in CAH supports the concept of StAR-independent pathways that can substitute for StAR deficiency. Thus STARD4 or STARD6 proteins could potentially provide low levels of StAR-independent cholesterol transfer into the mitochondria, but are not able to fully substitute for the level of StAR activity, because if they could then untreated CAH would not be lethal. In addition, the brain and placenta exhibit StAR-independent steroidogenesis (Miller 1997; Bose et al. 1996; Mellon 1994).

In summary, STARD4 and STARD6 proteins can transfer cholesterol intracellularly. Their function may also extend to transferring cholesterol into the mitochondria in steroidogenic cells for the purposes of enhancing *de novo* steroidogenesis (LaVoie et al. 2014; Soccio et al. 2005). The presence of STARD4 and STARD6 in ovarian steroidogenic cells lends support to the idea that these molecules could participate in steroidogenesis. Future studies could knockdown these molecules to determine their ability to contribute to endogenous steroidogenesis in ovarian or other steroidogenic cell types. Future subcellular fractionation studies including isolation of

mitochondria, mitochondrial associated membranes, endoplasmic reticulum, and plasma membrane fractions could provide further evidence for a role in steroid synthesis or other cholesterol-requiring cellular events.

## References

- Achleitner, GB, Gaigg, AK, Kainersdorfer, E, Kohlwein, SD, Perktold, A, Zellnig, G, and Daum, G. 1999. Association between the Endoplasmic Reticulum and Mitochondria of Yeast Facilitates Interorganelle Transport of Phospholipids through Membrane Contact. *European Journal of Biochemistry* 264 (2): 545–53. doi:10.1046/j.1432-1327.1999.00658.x.
- Alpy, F, and Tomasetto, C. 2005. Give Lipids a START: The StAR-Related Lipid Transfer (START) Domain in Mammals. *Journal of Cell Science* 118 (13): 2791–2801. doi:10.1242/jcs.02485.
- Alpy, F, and Tomasetto, C. 2014. START Ships Lipids across Interorganelle Space. *Biochimie, Lipids in Metabolic Diseases*, 96: 85–95. doi:10.1016/j.biochi.2013.09.015.
- Anttonen, M. 2002. FOG-2 and GATA-4 Are Coexpressed in the Mouse Ovary and Can Modulate Mullerian-Inhibiting Substance Expression. *Biology of Reproduction* 68 (4): 1333–40. doi:10.1095/biolreprod.102.008599.
- Bose, HS, Whittal, RM, Ran, Y, Bose, M, Baker, BY, and Miller, WL. 2008. StAR-like Activity and Molten Globule Behavior of StARD6, A Male Germ-Line Protein. *Biochemistry* 47 (8): 2277–88. doi:10.1021/bi701966a.
- Bose, HS, Sugawara, T, Strauss JF III & Miller WL. 1996. The pathophysiology and genetics of congenital lipid adrenal hyperplasia. *New England Journal of Medicine*. 335:1870–1878
- Caballero, F, Fernández, A, Lacy, AMD, Fernández-Checa, JC, Caballería, J, and García-Ruiz, C. 2009. Enhanced Free Cholesterol, SREBP-2 and StAR Expression in Human NASH. *Journal of Hepatology* 50 (4): 789–96. doi:10.1016/j.jhep.2008.12.016.
- Calderon-Dominguez, M, Gil, G, Medina, MA, Pandak, WM, and Rodríguez-Agudo, D. 2014. The StarD4 Subfamily of Steroidogenic Acute Regulatory-Related Lipid Transfer (START) Domain Proteins: New Players in Cholesterol Metabolism. *The International Journal of Biochemistry & Cell Biology* 49 (April): 64–68. doi:10.1016/j.biocel.2014.01.002.
- Caron, KM, Soo, S-C, Wetsel, WC, Stocco, DM, Clark, BJ, and Parker, KL. 1997. Targeted Disruption of the Mouse Gene Encoding Steroidogenic Acute Regulatory Protein Provides Insights into Congenital Lipoid Adrenal Hyperplasia. *Proceedings of the National Academy of Sciences* 94 (21): 11540–45.
- Chang, IY, Jeon, YJ, Jung, SM, Jang, YH, Ahn, JB, Park, KS and Yoon, SP. 2010. Does the StarD6 Mark the Same as the StAR

- in the Nervous System? *Journal of Chemical Neuroanatomy* 40 (3): 239–42. doi:10.1016/j.jchemneu.2010.06.006.
- Cherradi, N, Chambaz, EM, and Defaye, G. 1995. Organization of 3 Beta-Hydroxysteroid Dehydrogenase/isomerase and Cytochrome P450<sub>scc</sub> into a Catalytically Active Molecular Complex in Bovine Adrenocortical Mitochondria. *The Journal of Steroid Biochemistry and Molecular Biology* 55 (5-6): 507–14.
- Cherradi, N, Defaye, G, and Chambaz, EM. 1994. Characterization of the 3 Beta-Hydroxysteroid Dehydrogenase Activity Associated with Bovine Adrenocortical Mitochondria. *Endocrinology* 134 (3): 1358–64. doi:10.1210/endo.134.3.8119176.
- Clark, BJ. 2012. The Mammalian START Domain Protein Family in Lipid Transport in Health and Disease. *Journal of Endocrinology* 212 (3): 257–75. doi:10.1530/JOE-11-0313.
- Clark, BJ, Wells, J, King, SR, and Stocco, DM. 1994. The Purification, Cloning, and Expression of a Novel Luteinizing Hormone-Induced Mitochondrial Protein in MA-10 Mouse Leydig Tumor Cells. Characterization of the Steroidogenic Acute Regulatory Protein (StAR). *Journal of Biological Chemistry* 269 (45): 28314–22.
- DeAngelis, AM, Roy-O'Reilly, M, and Rodriguez, A. 2014. Genetic Alterations Affecting Cholesterol Metabolism and Human Fertility. *Biology of Reproduction*, August. doi:10.1095/biolreprod.114.119883.
- Definitions of Infertility and Recurrent Pregnancy Loss: A Committee Opinion. 2013. *Fertility and Sterility* 99 (1): 63. doi:10.1016/j.fertnstert.2012.09.023.
- Devoto, L, Christenson, LK, McAllister, JM, Makrigiannakis, A and Strauss, JF. 1999. Insulin and Insulin-like Growth Factor-I and- II Modulate Human Granulosa-lutein Cell Steroidogenesis: Enhancement of Steroidogenic Acute Regulatory Protein (StAR) Expression. *Molecular Human Reproduction* 5 (11): 1003–10. doi:10.1093/molehr/5.11.1003.
- Du, X, Brown, AJ, and Yang, H. 2015. Novel Mechanisms of Intracellular Cholesterol Transport: Oxysterol-Binding Proteins and Membrane Contact Sites. *Current Opinion in Cell Biology*, Cell organelles, 35 (August): 37–42. doi:10.1016/j.ceb.2015.04.002.
- Furukawa, A, Miyatake, A, Ohnishi, T, and Ichikawa, Y. 1998. Steroidogenic Acute Regulatory Protein (StAR) Transcripts Constitutively Expressed in the Adult Rat Central Nervous System: Colocalization of StAR, Cytochrome P-450<sub>SCC</sub> (CYP XIA1), and 3 $\beta$ -Hydroxysteroid Dehydrogenase in the Rat Brain. *Journal of Neurochemistry* 71 (6): 2231–38. doi:10.1046/j.1471-4159.1998.71062231.x.
- Garbarino, J, Pan, M, Chin, HF, Lund, FW, Maxfield, FR, and Breslow, JL. 2012. STARD4 Knockdown in HepG2 Cells Disrupts Cholesterol Trafficking Associated with the Plasma Membrane, ER, and ERC. *Journal of Lipid Research* 53 (12): 2716–25. doi:10.1194/jlr.M032227.
- Gillio-Meina C, Hui, YY, LaVoie, HA. GATA-4 and GATA-6 transcription factors: expression, immunohistochemical localization, and possible function in the porcine ovary. *Biol Reprod* 2003; 68: 412–22
- Goldstein, JL, DeBose-Boyd, RA, and Brown, MS. 2006. Protein Sensors for Membrane Sterols. *Cell* 124 (1): 35–46. doi:10.1016/j.cell.2005.12.022.

- Gomes, Cynthia, Oh, S-D, Kim, J-W, Chun, S-Y, Lee, K, Kwon, H-B, and Soh, J. 2005. Expression of the Putative Sterol Binding Protein Stard6 Gene Is Male Germ Cell Specific. *Biology of Reproduction* 72 (3): 651–58. doi:10.1095/biolreprod.104.032672.
- Helle, SCJ, Kanfer, G, Kolar, K, Lang, A, Michel, AH and Kornmann, B. 2013. Organization and Function of Membrane Contact Sites. *Biochimica et Biophysica Acta (BBA) - Molecular Cell Research*, Functional and structural diversity of the endoplasmic reticulum, 1833 (11): 2526–41. doi:10.1016/j.bbamcr.2013.01.028.
- Henry, Gray. *Gray's Anatomy of the Human Body*. Revised by Lewis, WH. New York: BARJLEBY. Com, 2000.
- Hylemon, PB, Pandak, WM, Vlahcevic, ZR. (2001) *Regulation of hepatic cholesterol homeostasis. in The Liver Biology and Pathobiology, eds Arias IM, Boyer JL, Chisari FV, Fausto N, Schachter DA, Shafritz DA. (Lippincott Williams & Wilkins, New York), 4th ed. pp 231–247.*
- Ikonen, E. 2008. Cellular Cholesterol Trafficking and Compartmentalization. *Nature Reviews Molecular Cell Biology* 9 (2): 125–38. doi:10.1038/nrm2336.
- Infertility | Reproductive Health | CDC. 2015. Accessed October 7. <http://www.cdc.gov/reproductivehealth/Infertility/>.
- John, ME, John, MC, Boggaram, V, Simpson, ER and Waterman, MR. 1986. Transcriptional Regulation of Steroid Hydroxylase Genes by Corticotropin. *Proceedings of the National Academy of Sciences of the United States of America* 83 (13): 4715–19.
- Jo, Youngah. King, SR, Khan, SA, and Stocco, DM. 2005. Involvement of Protein Kinase C and Cyclic Adenosine 3',5'-Monophosphate-Dependent Kinase in Steroidogenic Acute Regulatory Protein Expression and Steroid Biosynthesis in Leydig Cells. *Biology of Reproduction*. 73, 244–255. DOI 10.1095/biolreprod.104.037721.
- Kraemer, FB, Tavangar, K, and Hoffman, AR. 1991. Developmental Regulation of Hormone-Sensitive Lipase mRNA in the Rat: Changes in Steroidogenic Tissues. *Journal of Lipid Research* 32 (8): 1303–10.
- LaVoie, HA, and King, SR. 2009. Transcriptional Regulation of Steroidogenic Genes: STARD1, CYP11A1 and HSD3B. *Experimental Biology and Medicine* 234 (8): 880–907. doi:10.3181/0903-MR-97.
- LaVoie, HA, Whitfield, NE, Shi, B, King, SR, Bose, HS, and Hui, YY. 2014. STARD6 Is Expressed in Steroidogenic Cells of the Ovary and Can Enhance de Novo Steroidogenesis. *Experimental Biology and Medicine* 239 (4): 430–35. doi:10.1177/1535370213517616.
- Lebiedzinska, M, Szabadkai, G, Jones, AWE, Duszynski, J, and Wieckowski, MR. 2009. Interactions between the Endoplasmic Reticulum, Mitochondria, Plasma Membrane and Other Subcellular Organelles. *The International Journal of Biochemistry & Cell Biology*, Mitochondrial Dynamics and Function in Biology and Medicine, 41 (10): 1805–16. doi:10.1016/j.biocel.2009.02.017.
- Levine, T. 2004. Short-Range Intracellular Trafficking of Small Molecules across Endoplasmic Reticulum Junctions. *Trends in Cell Biology* 14 (9): 483–90. doi:10.1016/j.tcb.2004.07.017.

- Lev, S. 2010. Non-Vesicular Lipid Transport by Lipid-Transfer Proteins and Beyond. *Nature Reviews. Molecular Cell Biology* 11 (10): 739–50. doi:10.1038/nrm2971.
- Lin, D, Sugawara, T, Strauss, JF, Clark, BJ, Stocco, DM, Saenger, P, Rogol, A, and Miller, WL. 1995. Role of Steroidogenic Acute Regulatory Protein in Adrenal and Gonadal Steroidogenesis. *Science (New York, N.Y.)* 267 (5205): 1828–31.
- Majewska, MD, Harrison, NL, Schwartz, RD, Barker, JL, and Paul, SM. 1986. Steroid Hormone Metabolites Are Barbiturate-Like Modulators of the GABA Receptor. *Science, New Series*, 232 (4753): 1004–7.
- Manna, PR, Wang, X-J, and Stocco, DM. 2003. Involvement of Multiple Transcription Factors in the Regulation of Steroidogenic Acute Regulatory Protein Gene Expression. *Steroids* 68 (14): 1125–34. doi:10.1016/j.steroids.2003.07.009.
- Marchler-Bauer A et al. (2015), *CDD: NCBI's conserved domain database*. **Nucleic Acids Res.**43(D)222-6.
- Mascarenhas, MN, Flaxman, SR, Boerma, T, Vanderpoel, S and Stevens, GA. 2012. National, Regional, and Global Trends in Infertility Prevalence Since 1990: A Systematic Analysis of 277 Health Surveys. *PLoS Med* 9 (12): e1001356. doi:10.1371/journal.pmed.1001356.
- Mellon SH. 1994 Neurosteroids: biochemistry, modes of action, and clinical relevance. *Journal of Clinical Endocrinology and Metabolism*. 78:1003–1008.
- Mellon, SH., and Vaisse, C. 1989. cAMP Regulates P450<sub>scc</sub> Gene Expression by a Cycloheximide-Insensitive Mechanism in Cultured Mouse Leydig MA-10 Cells. *Proceedings of the National Academy of Sciences of the United States of America* 86 (20): 7775–79.
- Mesmin, B, Pipalia, NH, Lund, FW, Ramlall, TF, Sokolov, A, Eliezer, D, and Maxfield, FR. 2011. STARD4 Abundance Regulates Sterol Transport and Sensing. *Molecular Biology of the Cell* 22 (21): 4004–15. doi:10.1091/mbc.E11-04-0372.
- Mescher, Anthony L. Chapter 22. The Female Reproductive System. *Junqueira's Basic Histology: Text & Atlas, 13e*. Ed. Anthony L. Mescher. New York, NY: McGraw-Hill, 2013. n. pag. AccessMedicine. Web. NaN undefined NaN. <<http://accessmedicine.mhmedical.com.proxy.med.sc.edu/content.aspx?bookid=574&Sectionid=42524608>>.
- Miller, WL. 2007. Steroidogenic acute regulatory protein (StAR), a novel mitochondrial cholesterol transporter. *Biochimica et Biophysica Acta*. 1771 (2007) 663–676. [www.elsevier.com/locate/bbalip](http://www.elsevier.com/locate/bbalip)
- Miller, WL, and Auchus, RJ. 2011. The Molecular Biology, Biochemistry, and Physiology of Human Steroidogenesis and Its Disorders. *Endocrine Reviews* 32 (1): 81–151. doi:10.1210/er.2010-0013.
- Miller, WL and Bose, HS. 2011. Early Steps in Steroidogenesis: Intracellular Cholesterol Trafficking. *Journal of Lipid Research* 52 (12): 2111–35. doi:10.1194/jlr.R016675.
- Miller, WL. 1988. Molecular Biology of Steroid Hormone Synthesis. *Endocrine Reviews* 9 (3): 295–318. doi:10.1210/edrv-9-3-295.
- Miller, WL. 1997. Congenital Lipoid Adrenal Hyperplasia: The Human Gene Knockout for the Steroidogenic Acute Regulatory Protein. *Journal of Molecular Endocrinology* 19 (3): 227–40. doi:10.1677/jme.0.0190227.

- Montero, J, Morales, A, Llacuna, L, Lluís, JM, Terrones, O, Basañez, G, Antonsson, B. 2008. Mitochondrial Cholesterol Contributes to Chemotherapy Resistance in Hepatocellular Carcinoma. *Cancer Research* 68 (13): 5246–56. doi:10.1158/0008-5472.CAN-07-6161.
- NCBI. Homo Sapiens StAR-Related Lipid Transfer (START) Domain Containing 4 (STARD4), mRNA. 2014, February. [http://www.ncbi.nlm.nih.gov/nuccore/NM\\_139164.1](http://www.ncbi.nlm.nih.gov/nuccore/NM_139164.1).
- Papadopoulos, V, and Miller, WL. 2012. Role of Mitochondria in Steroidogenesis. *Best Practice & Research Clinical Endocrinology & Metabolism*, Mitochondria in Endocrinology, 26 (6): 771–90. doi:10.1016/j.beem.2012.05.002.
- Prasad, M, Kaur, J, Pawlak, KJ, Bose, M, Whittal, RM, and Bose, HS. 2014. Mitochondria-Associated Endoplasmic Reticulum Membrane (MAM) Regulates Steroidogenic Activity via Steroidogenic Acute Regulatory Protein (StAR)-Voltage-Dependent Anion Channel 2 (VDAC2) Interaction. *Journal of Biological Chemistry* 290 (5): 2604–16. doi:10.1074/jbc.M114.605808.
- Prinz, Will. 2002. Cholesterol Trafficking in the Secretory and Endocytic Systems. *Seminars in Cell & Developmental Biology* 13 (3): 197–203. doi:10.1016/S1084-9521(02)00048-4.
- Radhakrishnan, A, Goldstein, JL, McDonald, JG, and Brown, MS. 2008. “Switch-like Control of SREBP-2 Transport Triggered by Small Changes in ER Cholesterol: A Delicate Balance. *Cell Metabolism* 8 (6): 512–21. doi:10.1016/j.cmet.2008.10.008.
- Reinhart, MP, Billheimer, JT, Faust, JR, and Gaylor, JL. 1987. Subcellular Localization of the Enzymes of Cholesterol Biosynthesis and Metabolism in Rat Liver. *Journal of Biological Chemistry* 262 (20): 9649–55.
- Riegelhaupt, JJ, Waase, MP, Garbarino, J, Cruz, DE, and Breslow, JL. 2010. Targeted Disruption of Steroidogenic Acute Regulatory Protein D4 Leads to Modest Weight Reduction and Minor Alterations in Lipid Metabolism. *Journal of Lipid Research* 51 (5): 1134–43. doi:10.1194/jlr.M003095.
- Rodriguez-Agudo, D, Calderon-Dominguez, M, Ren, S, Marques, D, Redford, K, Medina-Torres, MA, Hylemon, P, Gil, G, and Pandak, WM. 2011. Subcellular Localization and Regulation of StarD4 Protein in Macrophages and Fibroblasts. *Biochimica et Biophysica Acta (BBA) - Molecular and Cell Biology of Lipids* 1811 (10): 597–606. doi:10.1016/j.bbalip.2011.06.028.
- Rodriguez-Agudo, D, Ren, S, Wong, E, Marques, D, Redford, K, Gil, G, Hylemon, P, and Pandak, WM. 2008. Intracellular Cholesterol Transporter StarD4 Binds Free Cholesterol and Increases Cholesteryl Ester Formation. *Journal of Lipid Research* 49 (7): 1409–19. doi:10.1194/jlr.M700537-JLR200.
- Romanowski, MJ, Soccio, RE, Breslow, JL, and Burley, SK. 2002. Crystal Structure of the Mus Musculus Cholesterol-Regulated START Protein 4 (StarD4) Containing a StAR-Related Lipid Transfer Domain. *Proceedings of the National Academy of Sciences* 99 (10): 6949–54. doi:10.1073/pnas.052140699.
- Rone, MB, Fan, J, and Papadopoulos, V. 2009. Cholesterol Transport in Steroid Biosynthesis: Role of Protein-Protein Interactions and Implications in Disease States. *Biochimica et Biophysica Acta* 1791 (7): 646–58. doi:10.1016/j.bbalip.2009.03.001.

- Rooyen, V, Derrick M, and Farrell, GC. 2011. SREBP-2: A Link between Insulin Resistance, Hepatic Cholesterol, and Inflammation in NASH. *Journal Of Gastroenterology And Hepatology* 26 (5): 789–92. doi:10.1111/j.1440-1746.2011.06704.x.
- Rusiñol, AE, Cui, Z, Chen, MH, and Vance, JE. 1994. A Unique Mitochondria-Associated Membrane Fraction from Rat Liver Has a High Capacity for Lipid Synthesis and Contains Pre-Golgi Secretory Proteins Including Nascent Lipoproteins. *Journal of Biological Chemistry* 269 (44): 27494–502.
- Seo and Lee. 2003. *Post-Translational Modifications and Their Biological Functions: Proteomic Analysis and Systemic Approches*. December 26.
- Simpson, E, Lauber, M, Demeter, M, Means, G, Mahendroo, M, Kilgore, M, Mendelson, C, and Waterman, M. 1992. Regulation of Expression of the Genes Encoding Steroidogenic Enzymes in the Ovary. *The Journal of Steroid Biochemistry and Molecular Biology* 41 (3-8): 409–13.
- Skiadas, CC, Duan, S, Correll, M, Rubio, R, Karaca, N, Ginsburg, ES, Quackenbush, J, and Racowsky, C. 2012. Ovarian Reserve Status in Young Women Is Associated with Altered Gene Expression in Membrana Granulosa Cells. *Molecular Human Reproduction* 18 (7): 362–71. doi:10.1093/molehr/gas008.
- Soccio, RE, Adams, RM, Maxwell, KN, and Breslow, JL. 2005. Differential Gene Regulation of StarD4 and StarD5 Cholesterol Transfer Proteins. Activation of StarD4 by Sterol Regulatory Element-Binding Protein-2 and StarD5 by Endoplasmic Reticulum Stress. *The Journal of Biological Chemistry* 280 (19): 19410–18. doi:10.1074/jbc.M501778200.
- Soccio, RE, Adams, RM, Romanowski, MJ, Sehayek, E, Burley, SK and Breslow, JL. 2002. The Cholesterol-Regulated StarD4 Gene Encodes a StAR-Related Lipid Transfer Protein with Two Closely Related Homologues, StarD5 and StarD6. *Proceedings of the National Academy of Sciences of the United States of America* 99 (10): 6943–48. doi:10.1073/pnas.052143799.
- Soccio, RE, and Breslow, JL. 2003. StAR-Related Lipid Transfer (START) Proteins: Mediators of Intracellular Lipid Metabolism. *Journal of Biological Chemistry* 278 (25): 22183–86. doi:10.1074/jbc.R300003200.
- Soccio, RE and Breslow, JL. 2004. Intracellular Cholesterol Transport. *Arteriosclerosis, Thrombosis, and Vascular Biology* 24 (7): 1150–60. doi:10.1161/01.ATV.0000131264.66417.d5.
- Stocco, DM 2000. The Role of the StAR Protein in Steroidogenesis: Challenges for the Future. *Journal of Endocrinology* 164 (3): 247–53. doi:10.1677/joe.0.1640247.
- Stocco, DM, and Clark, BJ. 1996. Regulation of the Acute Production of Steroids in Steroidogenic Cells. *Endocrine Reviews* 17 (3): 221–44. doi:10.1210/edrv-17-3-221.
- Stocco, DM. 2001. StAR Protein and the Regulation of Steroid Hormone Biosynthesis. *Annual Review of Physiology* 63 (1): 193–213. doi:10.1146/annurev.physiol.63.1.193.
- Stocco, DM, Clark, BJ, Reinhart, AJ, Williams, SC, Dyson, M, Dassi, B, Walsh, LP. 2001. Elements Involved in the Regulation of the StAR Gene. *Molecular and Cellular Endocrinology* 177 (1–2): 55–59. doi:10.1016/S0303-7207(01)00423-3.

- Stocco, DM, Wang, X, Jo, Y, and Manna, PR. 2005. Multiple Signaling Pathways Regulating Steroidogenesis and Steroidogenic Acute Regulatory Protein Expression: More Complicated than We Thought. *Molecular Endocrinology* 19 (11): 2647–59. doi:10.1210/me.2004-0532.
- Strauss, JF, Kishida, T, Christenson, LK, Fujimoto, T, and Hiroi, H. 2003. START Domain Proteins and the Intracellular Trafficking of Cholesterol in Steroidogenic Cells. *Molecular and Cellular Endocrinology* 202 (1-2): 59–65. doi:10.1016/S0303-7207(03)00063-7.
- Toulmay, A and Prinz, WA. 2011. Lipid Transfer and Signaling at Organelle Contact Sites: The Tip of the Iceberg. *Current Opinion in Cell Biology* 23 (4): 458–63. doi:10.1016/j.ceb.2011.04.006.
- Tremblay, JJ, Hamel, F, and Viger, RS. 2002. Protein Kinase A-Dependent Cooperation between GATA and CCAAT/Enhancer-Binding Protein Transcription Factors Regulates Steroidogenic Acute Regulatory Protein Promoter Activity. *Endocrinology* 143 (10): 3935–45. doi:10.1210/en.2002-220413.
- Vance, JE. 1990. Phospholipid Synthesis in a Membrane Fraction Associated with Mitochondria. *Journal of Biological Chemistry* 265 (13): 7248–56.
- Vance, JE. 2003. Molecular and Cell Biology of Phosphatidylserine and Phosphatidylethanolamine Metabolism. *Progress in Nucleic Acid Research and Molecular Biology* 75: 69–111.
- White, Bruce. *Endocrinology and Reproductive Physiology*, Edited by Susan porterfield. Philadelphia: Mosby, 2013.

# Appendix

## Appendix A: Permission to reuse figure 1.2

Rightslink® by Copyright Clearance Center Page 1 of 1

**RightsLink®**

[Home](#)[Create Account](#)[Help](#)[Live Chat](#)



**Title:** Transcriptional Regulation of Steroidogenic Genes: STARD1, CYP11A1 and HSD3B:  
**Author:** Holly A. LaVole, Steven R. King  
**Publication:** Experimental Biology and Medicine  
**Publisher:** SAGE Publications  
**Date:** 08/01/2009  
Copyright © 2009, © SAGE Publications

[LOGIN](#)

If you're a copyright.com user, you can login to RightsLink using your copyright.com credentials. Already a RightsLink user or want to [learn more?](#)

**Gratis Reuse**

Permission is granted at no cost for use of content in a Master's Thesis and/or Doctoral Dissertation. If you intend to distribute or sell your Master's Thesis/Doctoral Dissertation to the general public through print or website publication, please return to the previous page and select 'Republish in a Book/Journal' or 'Post on intranet/password-protected website' to complete your request.

[BACK](#)[CLOSE WINDOW](#)

Copyright © 2015 Copyright Clearance Center, Inc. All Rights Reserved. [Privacy statement](#). [Terms and Conditions](#). Comments? We would like to hear from you. E-mail us at [customercare@copyright.com](mailto:customercare@copyright.com)

https://s100.copyright.com/AppDispatchServlet

11/10/2015